ARTICLE

OBC
www.rsc.org/obc

Enzymatic cyclizations of squalene analogs with *threo*- and *erythro*-diols at the 6,7- or 10,11-positions by recombinant squalene cyclase. Trapping of carbocation intermediates and mechanistic insights into the product and substrate specificities†

Takamasa Abe and Tsutomu Hoshino*

Department of Applied Biological Chemistry, Faculty of Agriculture, and Graduate School of Science and Technology, Niigata University, Ikarashi, Niigata, 950-2181, Japan. E-mail: hoshitsu@agr.niigata-u.ac.jp; Fax: 81-25-262-6854

Received 11th May 2005, Accepted 21st June 2005
First published as an Advance Article on the web 27th July 2005

In order to trap the carbocation intermediates formed during the squalene cyclization cascade, squalene analogs with *threo*- and *erythro*-diols at the 6,7- and 10,11-positions were incubated with the recombinant squalene cyclase from *Alicyclobacillus acidocaldarius*, leading to the construction of the triterpenes with tetrahydropyran, octahydrochromene, decahydronaphthalene with a carbonyl group, dodecahydrobenzo[*f*]chromene, tetradecahydronaphtho[2,1-*b*]oxepine and malabaricane skeletons, almost of which are novel compounds. These products indicate that 6-membered monocyclic, 6/6-fused bicyclic and 6/6/5-fused tricyclic cations were involved in the cyclization reaction in addition to acyclic cation. All the trapped cations were the stable tertiary cation, but not the secondary one, indicating that the polycyclization reaction proceeds with a Markovnikov closure. The product profiles revealed that the cyclization reactions proceeded with the product and substrate specificities in addition to enantioselectivity. Mechanistic insight into the observed stereochemical specificities indicated that the pre-organized chair-conformation of squalene-diols is tightly constricted by the cyclase and a free motion or a conformational change is not allowed in the reaction cavity, thus, the substrate and product specificities are dominantly directed by the least motion of the nucleophilic hydroxyl group toward the intermediary carbocation; a small rotation of the hydroxyl group afforded the cyclization products in a good yield, but a large rotation of the hydroxyl group gave a marginal or no detectable amount of products.

Introduction

The enzymatic cyclizations of acyclic squalene **1** and 2,3-oxidosqualene to form polycyclic triterpenes have fascinated chemists and biochemists for over half a century.[1,2] X-Ray crystallographic analysis of prokaryotic squalene–hopene cyclase (SHC) was reported in 1997.[3] More recently, the three-dimensional structure of human lanosterol synthase was successfully elucidated.[4] SHC catalyses the conversion of **1** into the pentacyclic triterpenes of hopene **2** and hopanol **3**, the ratio being *ca.* 5 : 1, respectively (Scheme 1).[5,6] This polycyclization cascade is attained by a single enzyme. **1** is folded in all pre-chair conformation inside the reaction cavity and cyclized in a regio- and stereospecific manner through a series of carbocationic intermediates, leading to the formation of new five C–C bonds and nine chiral centers. Recent studies on the SHC from *Alicyclobacillus acidocaldarius* have revealed that the polycyclization reaction consists of 8 reaction steps (Scheme 1)[5]: (1) 1st cyclization to form A-ring **4** by proton attack on the terminal double bond, donated by the DXDD motif,[7] (2) 2nd ring closure to give the B-ring (6/6-fused A/B ring system **5**),[8,9] (3) 3rd cyclization to yield 5-membered C-ring (6/6/5-fused A/B/C-tricyclic ring system **6**) by Markovnikov closure,[9,10] (4) which then undergoes ring expansion to form the 6-membered C-ring (6/6/6-fused tricyclic ring system **7**),[10] (5) 5th cyclization to give the thermodynamically favored 5-membered D-ring (6/6/6/5-fused A/B/C/D ring system **8**, 17-*epi*-dammarenyl cation),[11–13] (6) followed by the second ring enlargement process to form the 6-membered D-ring (6/6/6/6-fused A/B/C/D-ring system, prohopanyl cation **9**),[11–14] (7) the last ring closure process to construct the 6/6/6/6/5-fused A/B/C/D/E-ring system

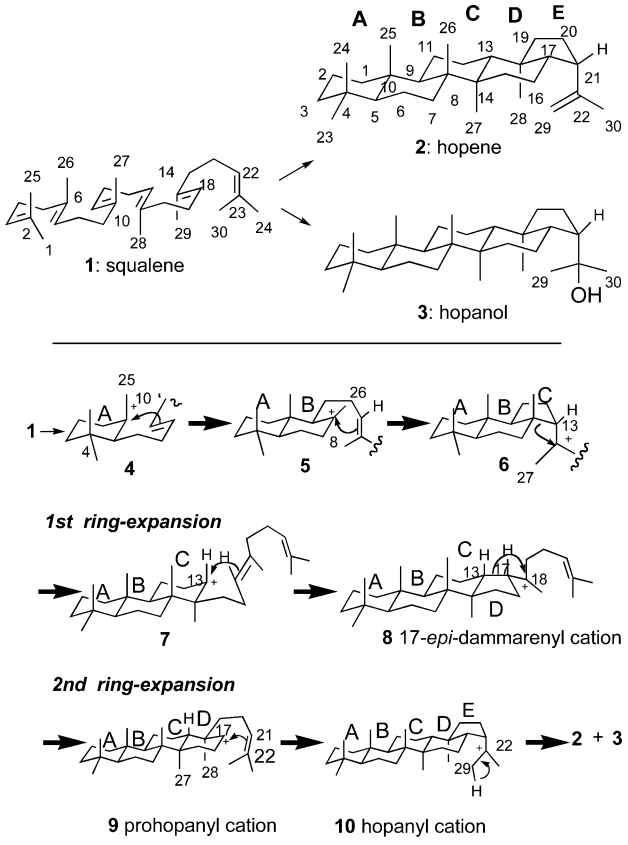

Scheme 1 Polycyclization pathway of squalene **1** to pentacyclic hopene **2** and hopanol **3**, which is presumed from the abortive cyclization products accumulated by the site-directed mutants.

† Electronic supplementary information (ESI) available: spectroscopic data. See http://dx.doi.org/10.1039/b506590a

DOI: 10.1039/b506590a

(**10**, hopanyl cation),[15] and (8) the final deprotonation reaction from **10** to introduce the double bond. Recently, Rajamani and Gao have given deeper insight into the polycyclization mechanism of **1**; they proposed that formation of **10** from **5** is achieved by a highly asynchronous concerted reaction and occurs by a kinetical preference.[16] The transient carbocations formed during the polycyclization cascade are stabilized by cation–π-interaction.[17] Previously, we clarified the roles of all the Trp residues conserved among prokaryotic SHCs,[18] and also demonstrated that cation–π interaction between π-electrons of aromatic amino acids and the transient carbocations made a great contribution to the acceleration of the polycyclization reaction at lower incubation temperatures. The replacement of Phe365,[8] Phe601[10] and Phe605[15a] by Tyr greatly enhanced the reaction velocity due to the elevated π-electron density of Tyr. In addition, a few tyrosine residues were shown to intensify the cation-π interaction by being placed at correct positions in the reaction cavity.[19–21] The steric bulk size of active site residues is likely to be responsible for stereochemical control during the polycyclization reaction; the substitution of Ile with smaller Ala or Gly at position 261 afforded false intermediates having 13α-H in the 6/6/5-fused tricyclic and 17α-H in the 6/6/6/5-fused tetracyclic cation,[14] the configurations of which are opposite to those of true intermediates **6** (13β-H) and **8** (17β-H) (Scheme 1). Replacement of Tyr420 or Leu607 by the bulkier Trp afforded unnatural monocyclic triterpene having (5*R*, 6*R*)-1,5,6-trimethylcyclohexene ring, named neoachillapentaene;[22] this cyclization proceeded *via* a constrained boat structure. This is the first example that **1** was folded into a boat structure despite the SHC adopting all chair structure. These findings indicate that the steric bulk size of active site residues direct the folding conformation of **1**, *i.e.*, the stereochemical destiny, during the polycyclization cascade.[5] Recently, we have clarified the catalytic mechanism for the final deprotonation reaction **10** → **2**.[23,24] Based on the X-ray analysis of *A. acidocaldarius* SHC,[3a] the catalytic base responsible for the deprotonation reaction has been suggested to be a water molecule (named a "front water"), the polarization of which is enhanced by other waters (named "back waters") that construct the hydrogen-bonding network by a combination of seven residues T41, E45, E93, R127, Q262, W133 and Y267.[3a,25] The "front water" thus polarized can store the proton generated from either Me-29 or Me-30 of hopanyl cation **10** to form **2** (Scheme 6, top), but **3** is produced if the "front water" adds as hydoxyl to the C-22 cation of **10** instead of accepting the proton.[3a,6,25] Recently, we have validate this proposal by the site-directed mutagenesis experiments.[23] The site-directed mutagenesis, targeted for the amino acids surrounding the "front water" such as Q262 and P263, resulted in a greatly enhanced production of **3** along with the decreased formation of **2**. A high production of **3** could be explained as follows. The point mutations could give rise to the perturbation around the "front water". This disordered "front water" can not act correctly as the catalytic base for the deprotonation reaction to form **2**, and in turn could be placed near to the final hopanyl cation **10**, leading to a high production of **3** without forming **2**.[23] The detailed polycyclization mechanism of squalene, described above, has been inferred from many site-directed mutagenesis experiments. Prokaryotic SHC is of particular note from the aspect of molecular evolution; deletion of Gly600 from the SHC altered the substrate specificity into that of eukaryotic oxidosqualene cyclases (OSCs), which is limited to (3*S*)-oxidosqualene.[26]

In addition, studies on the substrate analogs also have provided some important information for the reaction mechanism and the substrate recognition.[24,27–32] Previously, we reported the trapping experiments of the cationic intermediates. The truncated C_{22}-**11** and C_{27}-analogs **13** having an alcoholic group were efficiently cyclized into the carbocyclic skeleton with 6/6/5 + tetrahydrofuran (THF) ring **12**[5,10] and 6/6/6/5 + THF ring **14**,[5,12] respectively (Scheme 2), supporting that carbocationic

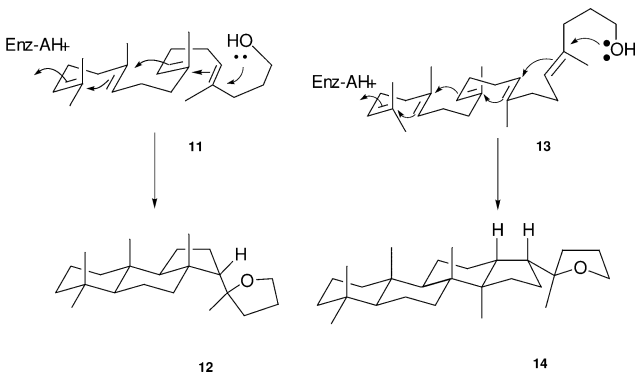

Scheme 2 Trappings of cationic intermediates **6** (6/6/5-fused tricycle) and **8** (6/6/6/5-fused tetracycle) by employing truncated squalene analogs **11** and **13** having a highly nucleophilic hydroxyl group.

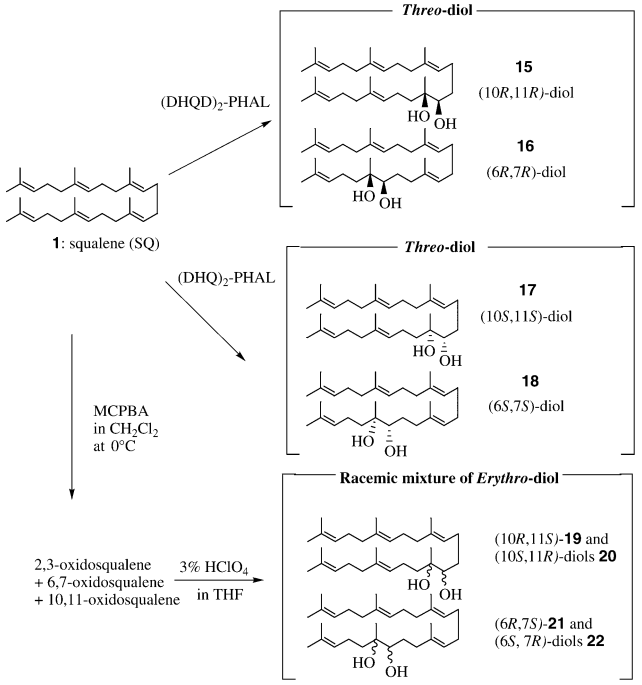

Scheme 3 Synthetic scheme of *threo* squalenediols **15**–**18** and *erythro* diols **19**–**22**. (10*R*, 11*R*)-**15** and (6*R*, 7*R*)-**16** were prepared with the chiral ligand of $(DHQD)_2$-PHAL, while (10*S*, 11*S*)-**17** and (6*S*, 7*S*)-**18** were with that of $(DHQ)_2$-PHAL. (3*R*)- and (3*S*)-2,3-squalenediols, which are produced in the reactions, are omitted in this scheme. To obtain the *erythro* diols, squalene **1** was treated with *m*-chloroperbenzoic acid (MCPBA) to afford oxidosqualenes having the epoxide at the (2,3)-, (6,7)- and (10,11)-positions, which are then subjected to hydrolysis with perchloric acid, giving the desired analogs. The *erythro* diols thus obtained are the racemic mixture of (10*R*, 11*S*)-**19** and (10*S*, 11*R*)-**20**, and that of (6*R*, 7*S*)-**21** and (6*S*, 7*R*)-**22**.

intermediates **6** and **8** are involved in the polycyclization reaction of **1**. To extend the trapping experiments of cationic intermediates, we synthesized *threo*-squalene diols, *e.g.*, 6,7-dihydroxy-**16** and **18**, 10,11-dihydroxysqualenes **15** and **17** in addition to the corresponding *erythro*-diols **19**–**22** (Scheme 3). By using the diol analogs, cationic intermediates **4**, **5** and **6** were successfully trapped. Moreover, these enzymic reactions were more or less accompanied by product and substrate specificities. The stereochemical analyses of the enzymic products demonstrated that the prefolded chair conformation of the analogs is rigidly constricted by squalene cyclase, thus a free motion or a conformational change of the folded chair structure is prohibited in the reaction cavity, once the polycyclization reaction starts, leading to the stereospecific construction of the triterpene skeleton. Herein, we describe the structures of the enzymic products and discuss the mechanism for the formation

of the enzymic products that were generated by incubating *threo*-diols **15**–**18** and *erythro*-diols **19**–**22** with squalene cyclase.

Results

Syntheses of *threo*-diols 15–18 and *erythro*-diols 19–22

The synthetic method is shown in Scheme 3. The asymmetric dihydroxylation of **1** was carried out using chiral ligands of $(DHQD)_2PHAL$ and $(DHQ)_2PHAL$, which were devised by Crispino and Sharpless.[33] The former ligand gives **15** and **16** having the (*R*, *R*)-stereochemistry, while the latter one affords **17** and **18** with the stereochemistry of (*S*, *S*). Isolation of **15**–**18** was carried out as follows. 2,3-Dihydroxysqualenes were concomitantly produced by the asymmetric dihydroxylation reactions. A SiO_2 column chromatography eluting with hexane–EtOAc (100 : 20) gave unreacted **1** and 2,3-dihydroxysqualenes in a pure state. A mixture of **15** and **16** was successfully separated with 5% $AgNO_3$–SiO_2 column chromatography by eluting with hexane–EtOAc (100 : 50). Isolation yields of 2,3-dihydroxysqualene, **15** and **16** were *ca.* 4, 7 and 6.5%, respectively. Analogs **17** and **18** were also obtained in similar yields. The enantiomeric excess (ee) of each diol was determined to be 88–95% based on the published values of optical rotation of each compound.[34] The *erythro*-analogs **19**–**22** were prepared as follows. **1** was treated with MCPBA and the epoxide rings was hydrolyzed with aqueous $HClO_4$, giving the racemic mixture of (10*R*, 11*S*)-**19** and (10*S*, 11*R*)-**20**, those of (6*R*, 7*S*)-**21** and (6*S*, 7*R*)-**22**, and (3*R*, *S*)-2,3-dihydroxysqualene, the separation of these *erythro*-diols was done with a similar method to that of the *threo*-diols.

Incubations of 15–22 with wild-type SHC and product profiles

Each of diols **15**–**22** (1 mg) was incubated with 2 cm^3 of the cell-free homogenates, which were prepared from an *E. coli* clone encoding the wild-type SHC. The incubation was carried out at optimal catalytic conditions (pH 6.0 and 60 °C) for 16 h and terminated by adding methanolic KOH (5%). The hexane extracts from the reaction mixture were subjected to a short SO_2 column chromatography eluting by hexane–EtOAc (100 : 30) in order to remove an excess of Triton X-100, which was included in the incubation mixture. Fig. 1 shows GC traces of the hexane extracts. As depicted in Fig. 1a, four products **23**, **24**, **25** and **26** were detected from *threo*-diol **15** in the distribution ratio of 2.2, 9.2, 61.3 and 19.3%, respectively, and the recovered **15** was 8.0%. Fig. 1b shows that diol **17** gave three products **27**, **28** and **29**, the product distribution being 61.9, 3.9 and 10.4%, respectively, along with the recovered **17** (23.8%). The GC peaks of **17** and **27** were overlapped, thus the distribution ratios were estimated by the HPLC separation. As seen in Fig. 1c, two compounds **30** (21.8%) and **31** (8.2%) were obtained from the reaction mixture of analog **16** in a moderate reaction yield (70% of **16** recovered). The cyclization reaction of diol **18** was poor (Fig. 1d) to afford one product **32** (10% yield), almost of **18** remained unchanged. The reaction yield was estimated by the separation of **32** and **18** with a SiO_2 column chromatography, because their GC peaks were overlapped (Fig. 1d). A mixture of *erythro*-diols **19** and **20** afforded **33** and **34** in distribution ratios of 15.2 and 29.8%, respectively, and the amount of the recovered analogs was 55.0% (Fig. 1e); as described in the Discussion section, **33** and **34** were produced only from diol **20** and no cyclization reaction occurred for diol **19** (Scheme 6). A racemic mixture of **21** and **22** afforded **35** and **36** in yields of 9.3 and 9.2%, respectively, and the recovered racemic mixture of **21** and **22** were 81.5%. As discussed later, this reaction was active only to **21**, but inert to **22** (Scheme 6).

Purification and structures of enzymic products 23–36

All the hexane extracts from the incubation mixture were passed through a short SiO_2 column in order to remove an excess amount of Triton X-100. Products **23**–**26** from diol **15** were partially purified by step-wise gradient elution (hexane–EtOAc, 100 : 3 → 100 : 10). For the complete separation of products **23**, **24** and **25**, HPLC was carried out eluting with hexane–2-PrOH (100 : 0.1). Product **26** was purified in a pure state by a

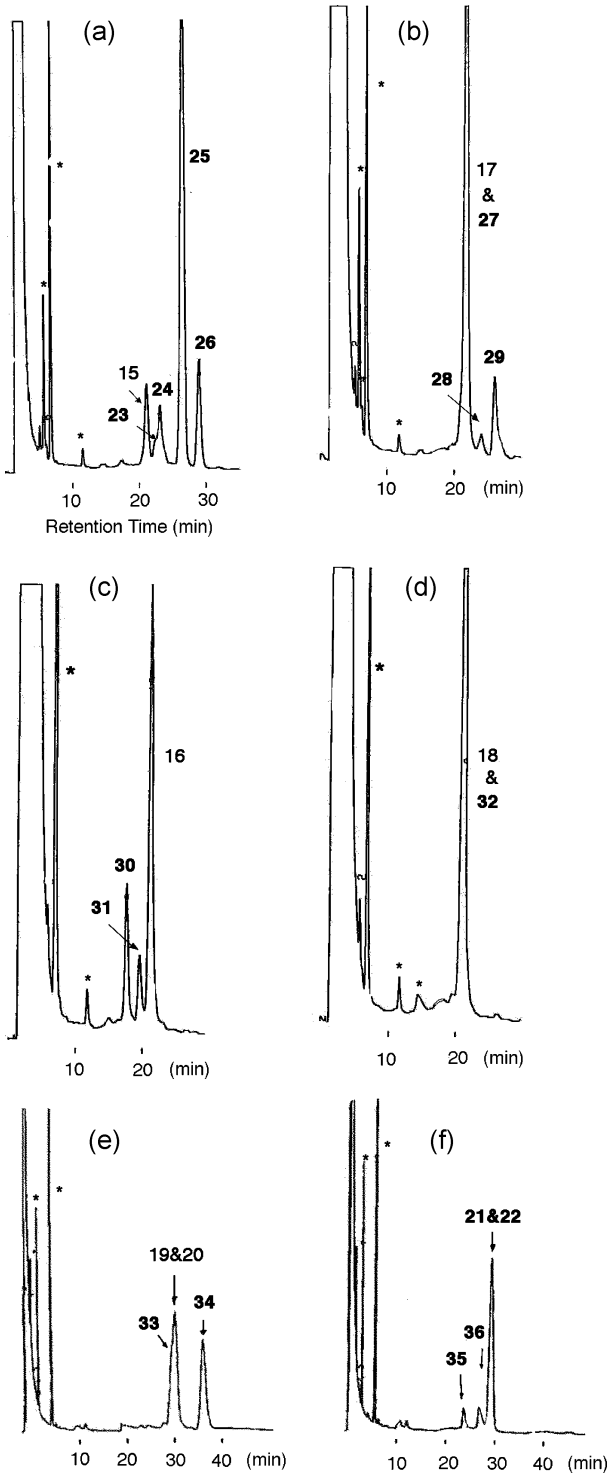

Fig. 1 Gas chromatograms of the hexane extracts from the incubation mixture of analogs **15**–**22** with the wild-type SHC. Triton X-100 included in the incubation mixture was removed by a short SiO_2 column eluting with hexane–EtOAc (100 : 30). (a) **15**, (b) **17**, (c) **16**, (d) **18**, (e) a racemic mixture of **19** and **20**, (f) a racemic mixture of **21** and **22**. The quantities of enzyme and the analogs used in each experiment (a–f) were identical: 2 cm^3 of the cell-free homogenates (equivalent to 0.4 mg of the pure SHC) and 1.0 mg of **15**–**22**. The asterisk symbols indicate the impurities. As shown in (b), (d) and (e), one of the enzymic products was inseparable from the diol substrates, thus the relative amounts of the products and the unreacted analogs were estimated by separating with SiO_2 column chromatography or HPLC.

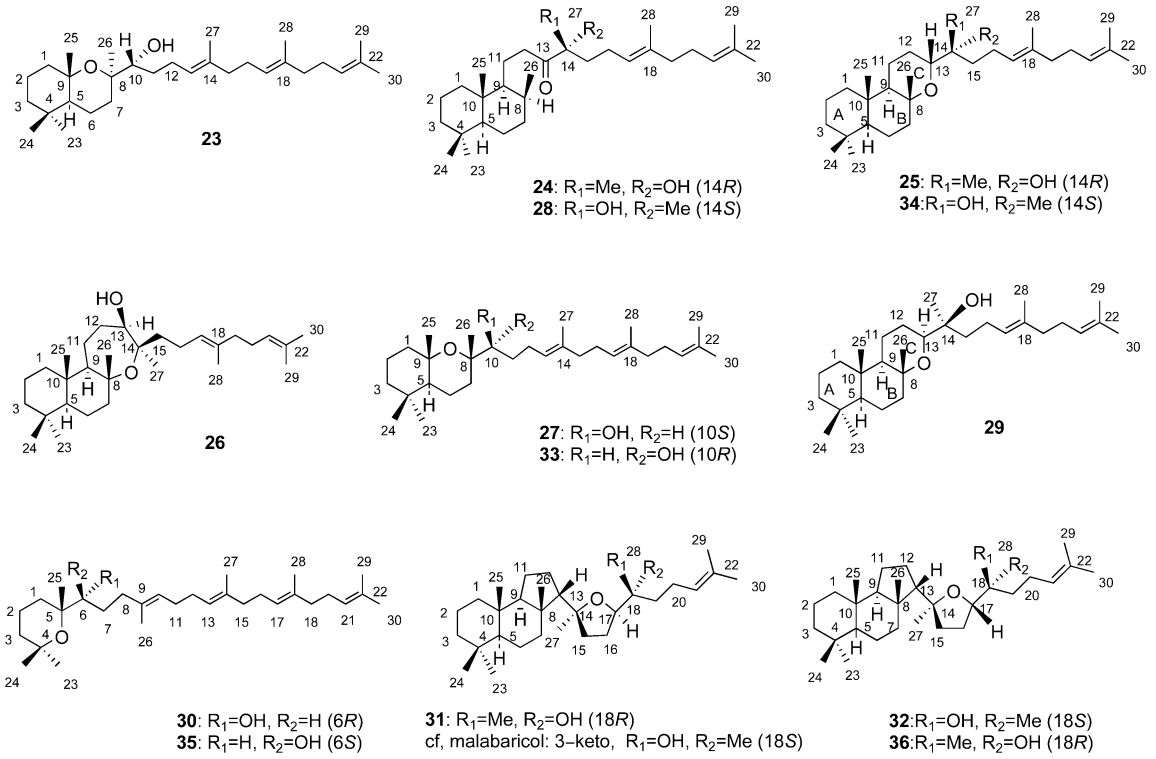

Fig. 2 Structures of the enzymic products **23**–**36**.

reversed phase HPLC (THF–H_2O = 3 : 2). Products from other diol substrates **16**–**18** were purified by a combination of normal and reversed phase HPLC, the composition and the ratio of the mixed solvent for the HPLC being hexane–2-PrOH (100 : 0.1) and THF–H_2O = 3 : 2, respectively. Separation of **27** and **29** was attained by the normal phase HPLC, but **28** was still impure. The complete purification of **28** was done by the reversed phase HPLC. Pure **31** was obtained by the normal HPLC, and the repetitive reversed phase HPLC gave pure **30**. Separation of product **32** and diol **18** was performed by the normal phase HPLC. Products **33** and **34**, from a racemic mixture of **19** and **20**, were purified as follows. **33** was isolated by the repetitive SiO_2 column chromatography (hexane–EtOAc = 100 : 1) and then the residues were subjected to the reversed phase HPLC (THF–H_2O = 1 : 1) to afford pure **34**. Products **35** and **36** obtained from diols **21** and **22** were homogeneously purified by the normal (hexane–2-PrOH = 100 : 0.05) and reverse phase HPLC (THF–H_2O = 1 : 1).

Structures of all the enzymic products were determined by detailed NMR analyses including DEPT, COSY 45, HOHAHA, NOESY, HMQC and HMBC. All the substrate analogs **15**–**22** contain five olefinic protons and seven allylic methyl groups. The ^{1}H NMR spectra of **23** showed the presence of three olefinic protons (δ_H 5.51, 5.44, 5.37, each 1H, t, J 6.4 or 7.0) and four allylic methyl groups (δ_H 1.69, 1.74, 1.81, 1.84, each 3H, s), while four methyl groups appeared at higher filed (δ_H 0.77, 0.90, 1.29 and 1.32, each 3H, s). In the HMBC spectrum, Me-25 (δ_H 1.32, 3H, s) and Me-26 (δ_H 1.29, 3H, s) had a correlation with C-9 (δ_C 75.4, s) and C-8 (δ_C 76.0, s), respectively, which suggested that a tetrahydropyran ring is involved. A clear NOE was observed between Me-26 and H-5 (δ_H 1.43, m), but no NOE of Me-25/Me-26, indicating the equatorial orientation of Me-26. Thus, **23** was determined to have bicyclic octahydrochromene structure as shown in Fig. 2. Product **27** also had a similar bicyclic structure, but the stereochemistry at C-8 was opposite to that of **23**; Me-25 (δ_H 1.27, 3H, s) of **27** had a strong NOE cross peak for Me-26 (δ_H 1.25, 3H, s). Interestingly, product **24** had a carbonyl group (δ_C 214.3, s), the position of which was determined to be at C-13 by a clear HMBC from Me-27 (δ_H 1.32, 3H, s). An apparent NOE between Me-25 (δ_H 0.926, 3H, s) and Me-26 (δ_H 0.975, 3H, d, J 7.2) indicated the axial orientation of Me-26. The detailed analyses of HMBC spectrum established that **24** is composed of a 6/6-fused bicyclic skeleton having a carbonyl group (Fig. 2). Product **28** had the same bicyclic skeleton with a carbonyl group as **24**, but the stereochemistry at C14 of **28** should be *S* in contrast to *R* of **24**, because (10*S*,11*S*)-**17** was used as the substrate. Tricyclic structures **25** and **29** were produced as the enzyme products from **15** and **17**, respectively. For **25**, an ether bond was found between C-8 (δ_C 74.9, s) and C-13 (δ_C 74.5, d), the assignments of which were determined by apparent HMBC cross peaks from Me-26 (δ_H 1.21, 3H, s) and Me-27 (δ_H 1.33, 3H, s), respectively. Detailed NMR analyses indicated that **25** had the 6/6/6-fused A/B/C tricyclic ring system, where the C-ring consists of a tetrahydropyran structure, thus dodecahydrobenzo[*f*]chromene skeleton was proposed as shown in Fig. 2. Detailed NMR analyses of product **29** also indicated the same tricyclic system as **25**. However, the stereochemistry at C-13 of **25** was opposite to that of **29**. A strong NOE between Me-26 (δ_H 1.21, 3H, s) and H-13 (δ_H 3.52, dd, J 11.6, 2.4) was observed for **25**, suggesting the axial orientation of H-13 in the chair structure. On the other hand, no observation of the NOE between them (Me-26, δ_H 1.18, 3H, s; H-13, δ_H 3.76, 1H, dd, J 12.4, 2.8) for **29** suggested the equatorial orientation for H-13 of **29**, but the large coupling constant (J 12.4) of the H-13 of **29** does not support the equatorial disposition. Molecular dynamics by Chem3D (Ver. 8.0, CambridgeSoft) indicated a boat structure for the C-ring, in which the dihedral angles between H-12 and H-13 were estimated to be about 170 and 53°, these values being consistent with the observed coupling constants (J 12.4, 2.8). Product **26** had a quite interesting structure consisting of the 6/6/7-fused A/B/C tricyclic ring system having the tetradecahydronaphtho[2,1-*b*]oxepine skeleton (Fig. 2). The ^{1}H NMR spectrum of **26** in acetone-d_6 clearly showed the presence of alcoholic proton (δ_H 3.37, d, J 6.0), which had the COSY cross peaks with H-13 (δ_H 3.67, t, J 6.0). An ether linkage was

found between C-8 (δ_C 80.28, s) and C-14 (δ_C 81.33, s). In the HMBC spectrum, Me-27 (δ_H 1.616, 3H, s) had cross peaks with C-14 and C-13 (δ_C 75.59, d), indicating that C(11)-OH of diol substrate **15** was employed for the ether bridge instead of C(10)-OH. Thus, **26** has the 7-membered oxepane skeleton. Indeed, the clear connectivity of H-12/H-11/H-9 was found in the COSY and HOHAHA spectra. Protons of H-13 and Me-27 were arranged in α-disposition, because strong NOEs were observed between O*H* at C-13 and Me-26 (δ_H 1.336, 3H, s) and between H-7 (δ_H 1.57, m) and Me-27, but no NOE between Me-26 and Me-27. Further detailed NMR analyses proved that the complete structure of **26** is shown in Fig. 2. It should be noted that the enzyme product having the 7-membered C-ring was constructed only from (*R*, *R*)-**15**, but not from the antipode (*S*, *S*)-**17**.

Compounds **30** and **31** were produced from (6*R*, 7*R*)-**16** as shown in Fig. 1. The ^{1}H NMR spectrum of **30** dissolved in C_6D_6 showed four olefinic protons (δ_H 5.55, 5.45, 5.42, 5.37) and five allylic methyl protons (δ_H 1.79, 3H, s; 1.73, 6H, s; 1.69, 3H, s; δ_H 1.80, 3H, s), suggesting that one double bond of **16** was used for the cyclization reaction to afford a monocyclic skeleton. The chemical shift values of C-4 (δ_C 71.5, s) and C-5 (δ_C 75.8, s) verified that an ether linkage is intervenient between them. The alcoholic proton (δ_H 2.76, d, *J* 4.0) exhibited doublet pattern due to the spin coupling with H-6 (δ_H 3.48, m). Both C-5 and C-6 of **30** must be *R*-configuration, because (6*R*, 7*R*)-**16** was employed as the substrate. Thus, the complete structure of **30** is depicted in Fig. 2. Product **31** had only one double bond (δ_H 5.45, t, *J* 6.8, δ_C 125.7, d; δ_C 130.9, s). An ether linkage was found between C-14 (δ_C 89.95, s) and C-17 (δ_C 82.03, d), the assignment of the carbon signals having been determined by the HMBC cross peaks from Me-27 (δ_H 1.29, 3H, s) and Me-28 (δ_H 1.22, 3H, s), respectively. A strong HMBC correlation was observed between the hydroxyl proton (δ_H 2.13, s) and C-28 (δ_C 21.99, q). These data strongly support that **31** possesses 5-membered tetrahydrofuran (THF) ring, but does not involve the 6-membered tetrahydropyran ring. Detailed analyses of the HMBC spectrum clearly verified that both 6/6/5-fused tricyclic ring system and THF ring are involved in **31**. A strong NOE between Me-26 (δ_H 1.00, 3H, s) and H-13 (δ_H 1.78, m) indicated the β-orientation of H-13. Stereochemistry of the THF ring was determined as follows. The chiral center at C-17 must have *R*-configuration, because diol substrate **16** used in this experiment has (*R*, *R*)-stereochemistry. A clear NOE between Me-27 and H-17 (δ_H 3.72, dd, *J* 8.4, 6.4) proved that these protons are arranged in the same geometry, leading to α-orientation of Me-27 (*i.e.* 14*S*-stereochemistry) due to α-orientation of H-17 in the THF ring (*i.e.* 17*R*-configuration), as shown in Fig. 1. From (6*S*, 7*S*)-diol **18**, only one product **32** was obtained (Fig. 1d). Product **32** also consisted of both a 6/6/5-fused tricyclic ring system and a THF ring, which was revealed by detailed analyses of the HMBC spectrum. A clear NOE between Me-26 (δ_H 1.06. 3H, s) and H-13 (δ_H 1.87, m) indicated that H-13 of **32** is arranged in the same β-orientation as that of **31**. However, the orientation of Me-27 (δ_H 1.23, 3H, s) is opposite to that of H-17 (δ_H 3.71, dd, *J* 10.4, 4.6), because no NOE was found between them. Since the diol substrate used in this experiment was (6*S*, 7*S*)-**18**, the chiral center of C-17 must have *S*-stereochemistry. Thus, the stereochemistry at C-14 of **32** was determined to be *S* as shown in Fig. 2. When the spin–spin coupling constant of H-17/H-16 was compared between **31** and **32**, the following idea can be proposed: the C(17)-*S* configuration gives rise to a pair of large and small coupling constants (*J* 10.4, 4.6) as shown in the ^{1}H NMR spectrum of **32**, whereas the C(17)-*R* stereochemistry provides a set of nearly equivalent values (*J* 8.4, 6.4) as seen in that of **31**, often leading to triplet-like splitting pattern.[35]

From the racemic mixture of *erythro*-diols of (10*R*, 11*S*)-**19** and (10*S*, 11*R*)-**20**, products **33** and **34** were produced. Detailed analyses of the HMBC spectrum of **33** led to the bicyclic octahydrochromene structure like product **27**. Furthermore, the EI-MS spectrum of **33** was superimposable onto that of **27** (refer to the electronic supplementary information). A clear NOE between Me-25 (δ_H 1.31, 3H, s) and Me-26 (δ_H 1.23, 3H, s) indicated β-orientation of Me-26, verifying that the chiral center of C-8 has *S*-configuration. The proton chemical shift of H-10 of **33** was significantly different from that of **27**, compared to other proton signals; δ_H 3.43 for **27**, while δ_H 3.63 for **33**, indicating that **33** has C(10)*R*-configuration in contrast to that of **27**. Thus, product **33** was produced only from (10*S*, 11*R*)-**20**, not from the corresponding enantiomer (10*R*, 11*S*)-**19**. Product **34** showed the same EI-MS spectrum as **25** including the fragment ions (see the supplementary information). Detailed analyses of the NMR spectra in C_6D_6 verified that **34** has the 6/6/6-fused tricyclic skeleton (dodecahydrobenzo[*f*]chromene structure) like **25**. A strong NOE between Me-26 (δ_H 1.21, 3H, s) and H-13 (δ_H 3.51, dd, *J* 11.8, 2.2) showed the axial disposition of H-13, verifying the same C(13)-*R*-stereochemistry as that of **25**. This further indicates that the C(14)-stereochemistry must be *S*, because the substrate used for the incubation is *erythro*-diol. Thus, product **34** was obtained only from **20**, but not from **19**. It is inferable that the polycyclization reaction enantioselectively occurred; diol **20** only was active, but inert to the corresponding enantiomer **19**.

Products **35** and **36** were obtained by the incubation of a mixture of *erythro*-diols, (6*R*, 7*S*)-**21** and (6*S*, 7*R*)-**22**. EI-MS spectra of **35** and **36** were identical to those of **30** and **32**, respectively, suggesting that **35** and **36** are monocycle and tetracycle (6/6/5-fused tricycle + THF ring), respectively. Detailed analyses of the NMR spectra are in full accord with the proposed structures depicted in Fig. 2. In the NOESY spectrum of **35**, H-2 (δ_H 1.48, m, ax.) had clear cross peaks with Me-25 (δ_H 1.20, 3H, s) and Me-24 (δ_H 1.216, 3H, s), indicating that the Me-24 and Me-25 are arranged in axial orientation like **30**. Thus, the stereochemistry at the C-5 of **35** is *R*, leading to *S*-configuration at the C-6, because *erythro*-diol was used as the substrate. In the ^{1}H NMR spectrum of **36** in acetone-d_6, the signal of H-17 (δ_H 3.31) showed double–doublet splitting pattern (*J* 11.1 and 3.3), that is, consisted of a pair of large and small coupling constants. This indicates C(17)-*S* configuration, as described in a comparison of **31** with **32**, which is further indicative of C(18)-*R*, because *erythro*-diol was used as the substrate. No NOE was observed between Me-27 (δ_H 1.37, s) and H-17, suggested that H-17 and Me-27 was placed in an opposite direction. Thus, the stereochemistry of the THF ring of **36** was determined to be 14*S* and 17*S* as shown in Fig. 2.

It is noticeable that some signals of the cyclopentane and the THF rings involved in **31**, **32** and **36** did not appear in the ^{13}C NMR spectrum, suggesting that there was little tumbling motion of these rings (see spectroscopic data in the Experimental section and supporting information). Products **31**, **32** and **36** are classified as malabaricane triterpenes with a 6/6/5-fused tricyclic ring system. The structure of malabaricol,[36] which was isolated from the wood of *Ailanthus malabarica*, is quite similar to that of **31**; the structural differences are found only in the following two points: malabaricol has a carbonyl group at C(3) of **31** and the stereochemistry of C(18) is opposite to that of **31** (see the structures shown in Fig. 2). van Tamelen *et al.* reported the chemical synthesis of the 6/6/5-fused tricyclic malabaricatriene from 2,3-oxidosqualene by using a Lewis acid.[37] Sharpless also reported the first nonenzymatic synthesis of malabaricanediol (3β-hydoxymalabaricol); *erythro*-18,19-dihydroxysqualene-2,3-oxide was treated with picric acid in CH_3NO_2 and then allowed to stand for 22 h at ambient temperature, giving a malabaricanediol in a yield of 7%.[38] The structure of malabaricanediol has the similar fundamental skeleton as those of **31**, **32** and **36**, but the configurations of C-17 and C-18 have not been elucidated. Furthermore, malabaricanediol was reported to have 14*S*-stereochemistry by Sharpless, which was opposite to 14*R* configuration of malabaricol, **31**, **32** and **36**.

Discussion

Mechanistic insight into the formation of enzymic products 23–32 from *threo*-diols 15–18

By using *threo*-diols **15**–**18**, cationic intermediates **4**, **5** and **6** were successfully trapped. Products **23** and **27** indicate that monocyclic cation **4** is involved during the polycyclization cascade. Products **24**–**26**, **28** and **29** demonstrated the intermediacy of bicyclic cation **5**. The presence of tricyclic cation **6** is verified by production of **31** and **32**. Furthermore, the production of **30** showed that acyclic C2-cation **42** (Scheme 5) is involved in the cyclization reaction, which has not been demonstrated before. Thus, the trappings of the stable tertiary cations **4**–**6** and **40** were successful, but that of secondary cation **7** failed, suggesting a significantly longer lifetime of the tertiary cations than that of the secondary one. A ring expansion from 5- to 6-membered ring (**6** → **7**) is likely to occur through cation–π-interaction for the complete polycyclization cascade,[8,15a,17] although another cyclization mechanism has been proposed that the polycyclization reaction occurs under a concerted manner without violation of Markovnikov's rule.[16,39] The following results obtained from this study should be noted.

(1) The conversion yields of squalene-diols **15**–**18** were different. 10,11-Dihydroxysqualenes **15** and **17** gave high conversion ratios of 92 and 76.2%, respectively, but those of 6,7-dihydroxylsqualenes **16** and **18** were significantly low (10–30%).

(2) The 6/6/7-fused tricycle (**26**: 6/6-fused bicycle + oxepane ring, *i.e.*, tetradecahydronaphthooxepine skeleton) was generated from (10*R*, 11*R*)-diol **15**, but not from the corresponding enantiomer (10*S*, 11*S*)-diol **17**. In addition, the monocycle **30** with a tetrahydropyran ring was constructed from (6*R*, 7*R*)-diol **16**, but not from the antipode (6*S*, 7*S*)-diol **18**. Thus, the formation of these products was enantioselective.

(3) Both enantiomers of (10*R*, 11*R*)-**15** and (10*S*, 11*S*)-**17**, and those of (6*R*, 7*R*)-**16** and (6*S*, 7*S*)-**18** gave enzymic products with the same heterocyclic skeletons, but the product distribution markedly differed between their enantiomers. The cyclic skeletons produced from both enantiomers **15** and **17** were as follows: octahydrochromene skeleton (**23** and **27**), decahydronaphthalene ring having an additional carbonyl group (**24** and **28**), and dodecahydrobenzo[*f*]chromene (**25** and **29**). On the other hand, **16** and **18** gave 3-deoxymalabaricol skeleton (**31** and **32**) consisting of both carbocyclic 6/6/5-fused tricycle and heterocyclic THF ring. However, the product distribution of **15** was quite different from that of the corresponding enantiomer **17**. The production ratio of **25**, **26**, **24** and **23** from **15** was estimated to be 27.9 : 8.8 : 4.2 : 1, while that of **27**, **29**and **28** from **17** was 15.9 : 2.7 : 1. Diol **16** gave monocycle **30** and tricycle **31** in a ratio of 2.7 : 1 (higher yield of monocycle **30**), while the corresponding enantiomer **18** afforded only tricycle **32**. Thus, it is inferable that the cyclization reactions of **15**–**18** exhibited the product and substrate specificities, which are accompanied by stereochemical control.

Mechanistic insights into why and how these specificities occurred provide a better understanding of squalene cyclization mechanism. Acyclic **1** is folded in all pre-chair conformation in the reaction cavity, thus substrate analogs **15**–**18** should be folded as depicted in Schemes 4 and 5. Previously, we reported that the isopropylidene moiety is essential to the initiation of the polycyclization reaction.[24,27] Analogs **15**–**18** have the isopropylidene double bond at both terminal sides, thus the cyclization reactions can start from both left side (a) and right side (b), as shown in Schemes 4 and 5. Scheme 4A shows the mechanisms for the formations of products **23**–**26** from **15**. According to Scheme 1, **15** underwent the cyclization reaction to afford both bicyclic cation **37** (like **5**) from **15a** and monocyclic cation **38** (like **4**) from **15b**. Both 10- and 11-OH of **15** could attack on cation **37**. A nucleophilic attack of the 11*R*-OH on the C15-cation of **37** gave **25** (path *a*), while the attack of 10*R*-OH afforded product **26** (path *b*). The hydride shift of H-11 to the C15-cation of **37**, followed by the deprotonation from 11*R*-OH, afforded a carbonyl group (path *c*) to yield **26**. To the C6-cation of **38**, 10*R*-OH attacked to give **23** (path *d*). As described above, the yield of **25** was significantly higher than that of **23** (*ca.* 28-fold), suggesting that the nucleophilic attack of axial OH to cation **37** was more favorable than that of equatorial OH. This product specificity would be explained in terms of the rotation angle between the OH and the p-orbital of carbocation. The equatorial OH of cation **38** must be largely rotated through C11–C12 axis in the cyclase cavity to form **23** (180°), whereas, in case of the axial OH, only a small motion (60°) is enough for the production of **25** from cation **37**, resulting in a significantly higher production of **25** than that of **23**. Thus, the findings strongly indicate that a free motion or large conformational change of the pre-organized chair structures is not allowed in the reaction cavity due to the tight binding of the folded chair structures to the cyclase enzyme. A rotation angle of 10*R*-OH of **37** for the formation of **26** is also smaller compared to that for the production of **23** and the equatorial OH is close to the C-15 cation, leading to higher production of **26** by *ca.* 9-fold than that of **23**. However, the yield of **26** having the 7-membered ring was less by 3-fold than that of **25** with the 6-membered ring, possibly due to the more favorable formation of 6-membered ring than that of 7-membered ring. Further evidence that the least motion directs the product specificity was given also by the cyclization reaction of (10*S*, 11*S*)-diol **17** (Scheme 4B); the yield of bicyclic **27** was highest (61.9%) among all the products **27**–**29**, due to the least motion (60°). Both enantiomers of **15** and **17** afforded the similar octahydrochromene skeleton (**23**, **27**), but the yields were significantly different; the yield of **23** was negligible (2.2%) and less by 30-fold than that of **27**. This product specificity can be explained also in terms of the least motion of the OH group; only a small rotation (60°) of the axial 10*S*-OH of cation **40** is required for the formation of **27** (path *h*), but a large rotation (180°) of 10*R*-OH of **38** for the formation of **23**. The production of **29** from cation **39** (path *e*) was not high (10.4%), due to the large rotation of 11*S*-OH. Path *g* led to the formation of **28** *via* hydride shift of H-11 to the C15-cation of **39** in a way similar to the formation of **24**. Formation of naphthooxepine skeleton from **39** is expected to occur *via* path *f*, but no detectable amount of this skeleton was found in the incubation mixture, due to the requirement of a large motion of the axial 10-OH of **39**; 10*R*-OH of **37** is close to the C15-cation to give **26**, but 10*S*-OH of **39** is distant from the C15-cation.

A tetrahydropyran ring **30** was constructed from (6*R*, 7*R*)-diol **16**, but not from the corresponding enantiomer (6*S*, 7*S*)-**18** (see Scheme 5A–B). This enantioselectivity also can be explained in terms of the degree of motion of the OH group; only a small motion (60°) toward C2-cation of acyclic cation **42** (path *j*), but a large rotation (180°) toward C2-cation of cation **44** (path *l*), thus, no detectable amount of the monocyclic product with a tetrahydropyran ring was found in the reaction mixture of **18**. The production ratio of **30** to **31** was 2.7 : 1. As shown in Scheme 5A, 7*R*-OH of cation **41** must rotate more largely (180°, path *i*) to produce **31** than 6*R*-OH of cation **42** (60°, path *j*), leading to a less amount of **31**. (6*S*, 7*S*)-Diol **18** also afforded product **32** *via* the least motion (60°) of 7*S*-OH of cation **43**. It should be noted that both products **31** and **32** had 14*S*-stereochemistry (the numbering according to Fig. 2), strongly indicating that the C10-Me of tricyclic cations **41** and **43** is in the α-orientation during the polycyclization cascade (Scheme 5).

Insight into the formation of enzymic products 33–36 from *erythro*-diols 19–22

Next, we discuss the cyclization mechanism of *erythro*-diols **19**–**22**. The formation mechanism of **33** and **34** from the racemate (**19** + **20**) is shown in Scheme 6A. The product structures of **33** and

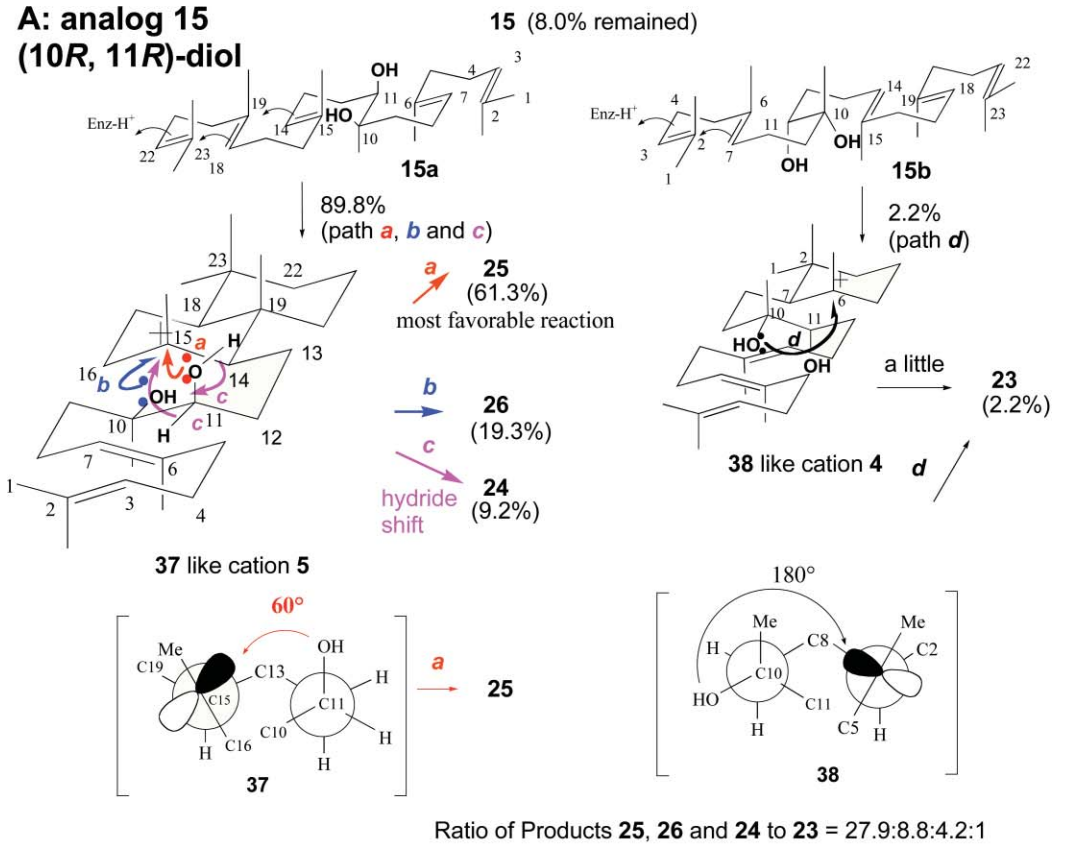

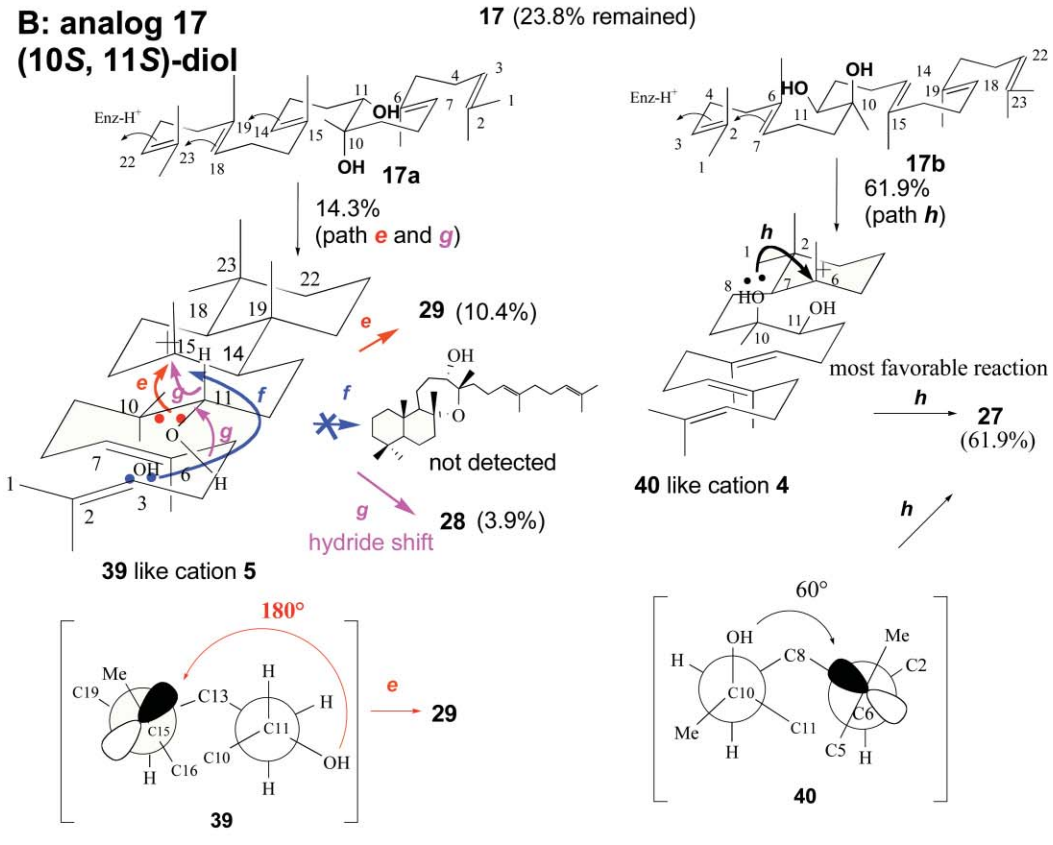

Scheme 4 (A) Mechanisms for the formation of products **23**–**26** from (10*R*, 11*R*)-diol **15** and (B) those of products **27**–**29** from (10*S*, 11*S*)-diol **17**.

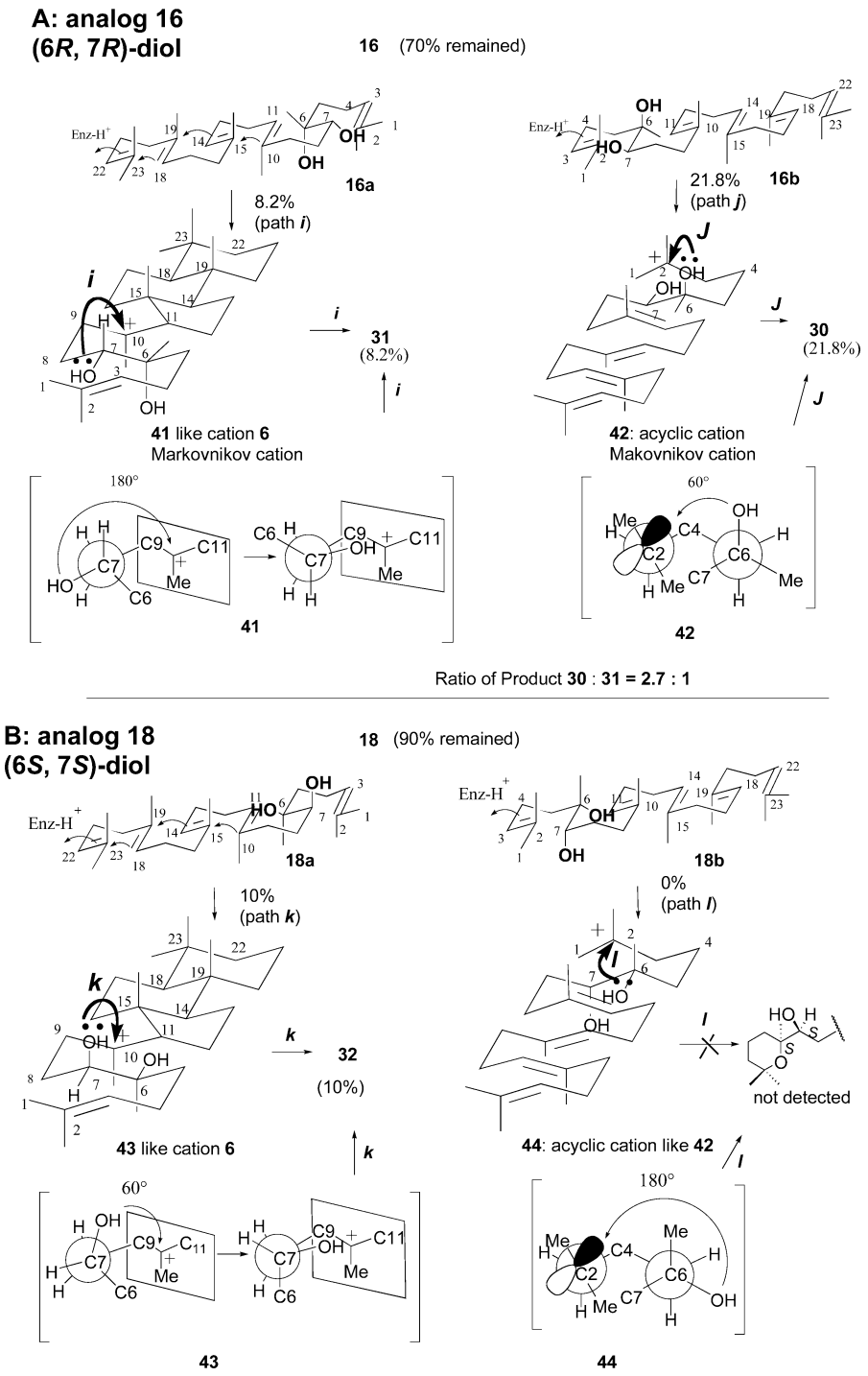

Scheme 5 (A) Mechanism for the formation of products **30** and **31** from (6*R*, 7*R*)-diol **16** and (B) that of **32** from (6*S*, 7*S*)-diol **18**.

34 (Fig. 2) clearly indicate that **20** only underwent the cyclization reaction, but the corresponding antipode **19** was not active, thus this reaction enantioselectively proceeded. Monocyclic **45** and bicyclic cations **46** could be converted to **33** and **34** *via* paths *m* and *n*, respectively, involving a least motion (60°), but no product from **19** was found due to the requirement of large rotation of the OH, as illustrated in Scheme 6A. The amount of **34** produced was *ca.* two-fold higher than that of **33**, indicating that bicyclic cation **46** was more easily formed than monocyclic cation **45**. The reason is not clear, but the steric bulk size of the large OH group may have affected the conversion yield, as discussed in the next section. The enantioselective cyclization was also found for the incubation of a racemic mixture of **21** and **22**, **21** was selectively converted to give **35** and **36** due to a small rotation (60°) of the OH (Scheme 6B), but **22** underwent no reaction due to the large rotation (180°). Thus, it is inferable that a motion degree of the nucleophilic OH group, irrespective of *threo*- and *erythro*-diols, dominantly determines the product and substrate specificities.

Effect of the bulk size of diols on the cyclization yields

Previously, we have demonstrated that the introduction of methyl group(s) at position(s) of C-7 and C-11 (the numbering starts from the initiation site of cyclization reaction) of the squalene backbone strongly prevents the formation of the chair-folding conformation inside the reaction cavity, leading to no reaction and/or to the early truncation of the polycyclization cascade.[29,32] This could possibly arise from the disorganization of the folded chair conformations as a result from the repulsive interaction of the methyl group(s) with the corresponding recognition site(s) of the cyclase.[29,32] Conformations **15b** and

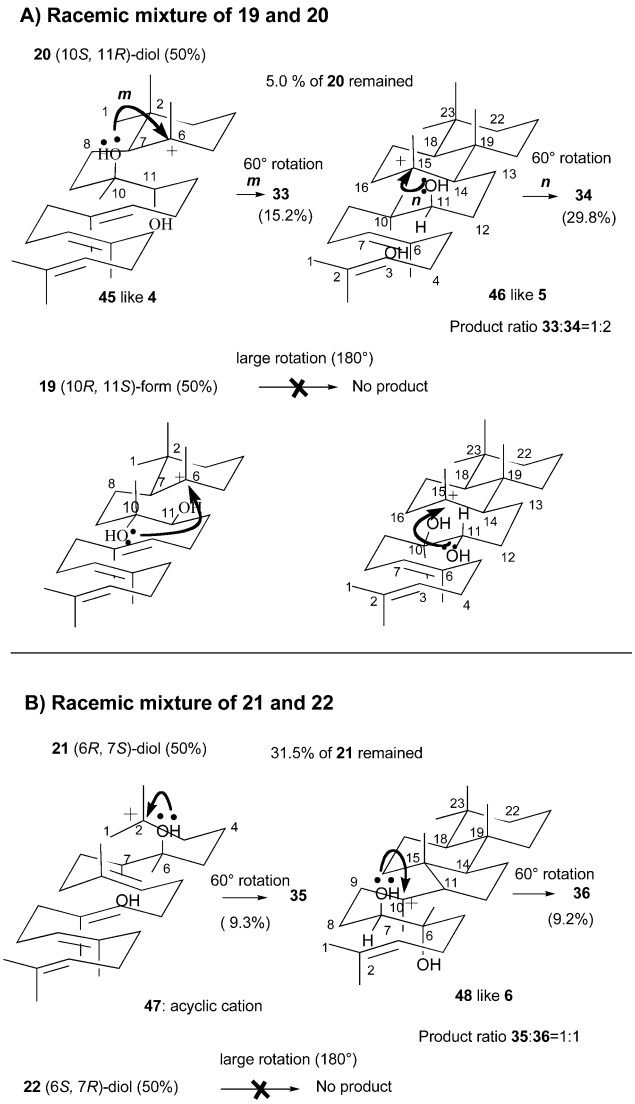

Scheme 6 (A) Cyclization of racemic mixture of *erythro*-diols **19** and **20** and (B) that of **21** and **22**.

18b have a bulky hydroxyl group at 11- or 7-position, which is arranged in an axial disposition. In addition to the large rotation angle of the OH (180°), which is required for the formation of **23** from **15b** and a terahydropyran ring from **18b**, the steric repulsive interaction of the bulky hydroxyl group with the cyclase may have disordered the pre-folded chair structure, resulting in a further decrease of the cyclization yields (2.2% for **15b** and 0% for **18b**). When the cyclization reactions of *erythro*-diols **20** and **21** were compared, the production of **34** was higher than that of **36** (*ca.* 3-fold), despite both products having been produced *via* a least motion of the OH (60°) (see Scheme 6), indicating that bicyclic cation **5** was more easily formed than tricyclic cation **6**. A more preferable formation of **5** was also found in a comparison of *threo*-diols of **15** and **18**; the production amount of **25** was remarkably larger (*ca.* 6-fold) than that of **32**, despite both products being generated *via* a least motion (60°) of the OH (see Schemes 4 and 5). These facts indicate that the cyclization yields depended not only on the rotation angle of the OH, but also on the steric bulk size of the substrate analog. The repulsive interaction of the bulky OH group at C7 of **43** and **48** with the cyclase would be larger compared to that of C11 of **37** and **46**, resulting in higher production of the bicyclic cation **5** than that of the tricyclic cation **6**. As described above, 10,11-diols **15** and **17** were more favorably accepted as the substrates than 6,7-diols **16** and **18**. On the other hand, 6,7-epoxysqualene afforded significantly higher conversion yield compared to 10,11-epoxysqualene (results to be published), indicating that, in the case of epoxysqualene, the formation of tricyclic cation **6** is more preferable than that of bicyclic cation **5**. This opposite feature between epoxide and diol would be due to the difference of their steric bulk sizes; the epoxide ring is smaller than that of diol. This finding also indicates that the bulkier hydroxyl groups more or less affected the formation of the rigidly held chair conformation, resulting in decreased cyclization yield. However, we can unambiguously conclude that the rotation angle of the nucleophilic OH group substantially directs the substrate and product specificities, as discussed in the previous sections.

In conclusion, we succeeded in trapping the intermediates of acyclic C2-cation, monocyclic **4**, bicyclic **5** and tricyclic cations **6** by using *threo*- and *erythro*-diols of squalene, demonstrating the significantly longer lifetime of these tertiary cations (Markovnikov cations) formed during the polycyclization cascade of **1**. The cyclization reactions proceeded with the product specificity and/or substrate specificity, which can be explained in terms of the motion degree of the nucleophilic hydroxyl group toward the intermediary carbocation. Thus, we have now the strong evidence that all the prefolded chair conformation is tightly constricted by the cyclase enzyme, thus, a free motion or a large conformational change of the folded chair conformation is not allowed inside the reaction cavity. Previously, Cornforth proposed that the protosterol cation has 17α-oriented side chain,[40] but in order to produce the 20*R*-stereochemistry of lanosterol, a 120° rotation of the side chain through the C17–C20 bond is required prior to the hydride shift from C17 to C20. In contrast, Corey proposed, based on studies of the substrate analogs, *e.g.* 20-oxa analog and (20*E*)-20,21-dehydro-analog of oxidosqualene, that the side chain at C17 of protosterol cation must be arranged in β-orientation, in which only a small rotation (<60°) around the C17–C20 bond is required,[41,42] thus Cornforth's rationalization of the conformational change to explain C20-*R* configuration is no longer necessary. Corey's idea indicates that the pre-organized chair–boat–chair conformation is tightly bound to the oxidosqualene cyclase and the conformational change is not allowed in the reaction cavity, which is in good accordance with the inference from the present investigations of squalene diols. Moreover, through these trapping experiments, novel triterpenes were created that have the skeletons of octahydrochromene, dodecahydrobenzo[*f*]chromene and tetradecahydronaphtho[2,1-*b*]oxepine, in addition to the production of natural triterpene skeleton of 3-deoxymalabaricol.

Experimental

Analytical methods

NMR spectra were mainly recorded in C_6D_6 on a Bruker DMX 600 or DPX 400 spectrometer, the chemical shifts being relative to the solvent peak δ_H 7.280 and δ_C 128.0 ppm as the internal reference for ^{1}H- and ^{13}C NMR spectra, respectively. Some synthetic intermediates were measured in $CDCl_3$. The chemical shifts in $CDCl_3$ solution were given according to the internal solvent peaks of δ_H 7.26 and δ_C 77.0 ppm. To further validate the proposed structures, the NMR data of some enzymic products were measured in acetone-d_6, the solvent peak being referred to be δ_H 2.04, δ_C 29.8 ppm. The coupling constants J are given in Hz. GC analyses were done on a Shimadzu GC-8A chromatograph equipped with a flame ionization detector (DB-1 capillary column, 0.53 mm × 30 m). GC-MS spectra were on a JEOL SX 100 spectrometer under electronic impact at 70 eV with a DB-1 capillary column (0.32 mm × 30 m), the oven temperature being elevated from 220 to 270 °C (3 °C min^{-1}). HR-EIMS was measured by direct inlet system. Specific rotation values were measured at 25 °C with a Horiba SEPA-300 polarimeter. FABMS (positive) including HRMS was measured using glycerol matrix.

Incubation condition and purification of enzymatic products

Standard incubation conditions were performed according to the published protocols.[7a,24] The cell-free homogenates were prepared as follows. A one liter culture of *E. coli* encoding the native SHC was harvested by centrifugation and to the collected pellets was added 50 cm^3 of citrate buffer solution (pH 6.0), and then subjected to ultrasonication to disrupt the cells. The supernatant was used for the incubations after removing the cell debris by centrifugation. One cm^3 of the supernatant contains *ca.* 200 μg of the pure SHC. The incubation mixtures were lyophilized, and then the products and the unreacted substrate analogs were extracted three times with a mixture of hexane and EtOAc (100 : 10). An excess of Triton X-100 detergent was removed by passing a short SiO_2 column eluting with hexane–EtOAc (100 : 20). Each product was purified by a combination of the normal and the reverse phase HPLC, as described in the text.

Syntheses of *threo*-squalene diols 15–18

These compounds were synthesized according to the published protocol. The flask (500 cm^3) containing 10 cm^3 of ^{t}BuOH–H_2O was well cooled to 0 °C. To the well-stirred solution, $(DHQD)_2PHAL$ (40 mg, 5.0 mol%), $K_3Fe(CN)_6$ (0.99 g, 3 mmol), K_2CO_3 (0.42 g, 3 mmol), $CH_3SO_2NH_2$ (96 mg, 1 mmol), OsO_4 (2.54 mg, 1.0 mol%) were added and further stirred for 30 min until almost of the reagents was dissolved. To the mixture was added squalene **1** (410 mg, 1 mmol), dissolved in a small amount of ^{t}BuOH. The reaction was further continued by stirring at 0 °C for 24 h, followed by addition of $Na_2S_2O_5$ (1.5 g, 7.9 mmol), and then warmed to room temperature. The diol mixture was extracted with EtOAc (50 cm^3 × 3). The organic layer was washed with 6 N aq. NaOH and dried over anhydrous Na_2SO_4 and stood overnight. After evaporating EtOAc under reduced pressure, the residues were subjected to a column chromatography over SiO_2. To isolate the desired materials, the following solvents were used. First, hexane was used to remove the unreacted starting material **1**. Second, by eluting with hexane–EtOAc (100 : 10), 2,3(*R*)-squalene diol was obtained in pure state, but the separation of **15** and **16** failed. $AgNO_3$-impregnated (5%) SiO_2 column chromatography led to the successful separation, giving the desired products in the following yields: 16.9 mg (3.8%) for 2,3(*R*)-squalene diol, 9.0 mg (2.0%) for **15** and 20.2 mg (4.6%) for **16**. Sufficient amounts of **16** and **17** for the present experiments were prepared by repeated and large-scale experiments. The specific rotations ($[a]_D^{25}$), of **15** and **16** were +10.44° (*c* 2.14, $CHCl_3$) and +10.23 (*c* 16.96, $CHCl_3$), respectively, indicating that the optical purities were 94.9 and 87% ee, respectively.[34] To prepare the *threo*-(*S*, *S*)-diols, $(DHQ)_2PHAL$ was used instead of $(DHQD)_2PHAL$, but the synthetic and isolation methods were essentially the same as those of the enantiomers. The specific rotations ($[a]_D^{25}$), for **18** and **17** were +10.33° (*c* 8.51, $CHCl_3$) and +9.75 (*c* 4.02, $CHCl_3$), respectively. Thus, the optical purities of **18** and **17** were 88.9 and 87.5% ee, respectively. The NMR and MS spectral data were indistinguishable between the (*R*, *R*)- and the (*S*, *S*)-forms, because of the enantiomeric relationship between them. NMR data of **15**–**18** are given in the ESI.

Syntheses of a mixture of *erythro*-(6*R*, 7*S*)-21 and (6*S*, 7*R*)-22, and that of *erythro*-(10*R*, 11*S*)-19 and (10*S*, 11*R*)-20

To the cooled solution of squalene (101.3 mg, 0.25 mmol) in CH_2Cl_2 (2.5 cm^3) at 0 °C, MCPBA (62.9 mg, 0.365 mmol) was added and stirred for 2 h. This reaction mixture was washed with 20% $NaHCO_3$ (10 cm^3 × 3) and with brine (10 cm^3 × 2), and the organic layer was dried over anhydrous Na_2SO_4. To remove the unreacted **1**, the reaction mixture was passed through a short SiO_2 column to afford 6,7-oxido- and 10,11-oxido- and 2,3-oxidosqualenes (total yield, 71.7%). To a mixture of the three oxidosqualenes (1.0 g) dissolved in THF (17.5 cm^3), was added 2 cm^3 of 3% perchloric acid and stirred for 3 h at ambient temperature. The reaction mixture was poured into the ice-water, then the products were extracted with hexane (500 cm^3 × 3), which was washed with 10% $NaHCO_3$ and with brine, then dried over anhydrous Na_2CO_3. The three squalene diols were partially separated by SiO_2 column chromatography. Complete separation was accomplished with 5% $AgNO_3$–SiO_2 column chromatography eluting with hexane–EtOAc (100 : 20). The yields were as follows: 0.28 g for the mixture of (10*R*, 11*S*)- and (10*S*, 11*R*)-squalene diol, 0.24 g for the mixture of (6*R*, 7*S*)- and (6*S*, 7*R*)-squalene diol, and 0.10 g for the mixture of (2, 3*R*)- and (2, 3*S*)-oxidosqualene. NMR data of the racemic mixture of (6*R*, 7*S*)-**21** and (6*S*, 7*R*)-**22** and that of (10*R*, 11*S*)-**19** and (10*S*, 11*R*)-**20** are given in the ESI.

Spectroscopic data of enzymic products 23–36

Product 23 (oil). NMR data in C_6D_6 (400 MHz): δ_H 0.775 (3H, s, H-24), 0.903 (3H, s, H-23), 1.21 (dd, *J* 12.8, 4.8, H-3), 1.29 (3H, s, H-26), 1.32 (3H, s, H-25), 1.34 (2H, m, H-2 & H-3), 1.39 (m, H-6), 1.43 (1H, m, H-5), 1.48 (m, H-2), 1.49 (m, H-7), 1.50 (2H, m, H-6 & H-11), 1.67 (m, H-11), 1.69 (3H, s, H-29), 1.74 (3H, s, H-28), 1.75 (m, H-1), 1.81 (3H, s, H-30), 1.84 (3H, s, H-27), 1.89 (m, H-7), 2.21 (2H, t, *J* 7.2, H-19), 2.22 (2H, t, *J* 7.2, H-15), 2.27 (2H, t, *J* 7.2, H-20), 2.33 (2H, t, *J* 7.2), 2.48 (m, H-1), 2.51 (m, H-12), 2.72 (m, H-12), 3.81 (d, *J* 10.0, H-10), 5.37 (t, *J* 6.4, H-21), 5.44 (t, *J* 6.4, H-17), 5.51 (t, *J* 7.0, H-13); δ_C 16.07 (C-6), 16.11 (C-28), 16.19 (C-27), 17.72 (C-29), 20.34 (C-2), 20.68 (C-24), 23.57 (C-25), 24.29 (C-26), 25.84 (C-30), 26.08 (C-12), 27.23 (C-16), 27.30 (C-20), 31.87 (C-7), 32.14 (C-23), 32.52 (C-11), 33.54 (C-4), 40.21 (C-15), 40.33 (C-19), 41.72 (C-3), 42.54 (C-1), 51.57 (C-5), 75.39 (C-9), 75.68 (C-10), 76.03 (C-8), 124.88 (C-17), 124.93 (C-21), 125.2 (C-13), 131.1 (C-22), 134.9 (C-18), 135.6 (C-14). The assignments of C-16 and C-20, and those of C-15 and C-19 are interchangeable. EIMS *m/z* (%): 69 (39), 81 (15), 95 (13), 109 (8), 137 (15), 177 (74), 195 (100), 444 (M^+, 1). HRFABMS (glycerol) *m/z* (M + H): calcd. for $C_{30}H_{53}O_2$, 445.4046; found 445.4122. $[a]_D^{25}$ = +26.1 (*c* 0.11, $CHCl_3$).

Product 24 (oil). NMR data in C_6D_6 (400 MHz): δ_H 0.905 (m, H-5), 0.926 (3H, s, H-25), 0.930 (m, H-1), 0.950 (3H, s, H-24), 0.975 (d, *J* 7.2, H-26), 1.01 (3H, s, H-23), 1.12 (m, H-9), 1.25 (ddd, 12.8, 12.8, 3.6, H-3), 1.32 (3H, s, H-27), 1.41 (m, H-2), 1.47 (2H, m, H-3 & H-6), 1.47 (m, H-3), 1.55 (m, H-2), 1.64 (2H, m, H-6 & H-7), 1.65 (m, H-11), 1.69 (3H, s, H-29), 1.70 (3H, s, H-28), 1.75 (m, H-7), 1.80 (m, H-1), 1.803 (3H, s, H-30), 1.86 (m, H-15), 2.03 (m, H-11), 2.07 (m, H-16), 2.18 (2H, t, *J* 6.8, H-19), 2.26 (m, H-15), 2.29 (2H, t, *J* 6.8, H-20), 2.30 (m, H-12), 2.39 (m, H-16), 2.43 (m, H-12), 5.31 (t, *J* 6.8, H-17), 5.34 (t, *J* 6.8, H-21); δ_C 15.44 (C-26), 16.04 (C-28), 16.45 (C-25), 17.71 (C-29), 17.76 (C-6), 18.76 (C-2), 20.52 (C-11), 21.79 (C-24), 22.70 (C-16), 25.75 (C-27), 25.82 (C-30), 27.08 (C-20), 29.82 (C-8), 33.45 (C-4), 33.70 (C-23), 34.45 (C-12), 34.99 (C-7), 38.75 (C-10), 39.72 (C-1), 40.04 (C-19), 40.16 (C-15), 42.34 (C-3), 53.03 (C-9), 56.87 (C-5), 78.61 (C-14), 124.1 (C-17), 124.8 (C-21), 131.3 (C-22), 135.9 (C-18), 214.3 (C-13). EIMS *m/z* (%): 69 (100), 81 (33), 95 (29), 109 (31), 137 (26), 177 (63), 294 (37), 444 (M^+, 1). HRFABMS (glycerol) *m/z* (M + H): calcd. for $C_{30}H_{53}O_2$, 445.4046; found: 445.4127. $[a]_D^{25}$ = +8.18 (*c* 0.275, $CHCl_3$).

Product 25 (oil). NMR data in C_6D_6 (400 MHz): δ_H 0.738 (3H, s, H-25), 0.780 (ddd, *J* 12.8,12.8,3.2, H-1), 0.888 (3H, s, H-24), 0.900 (m, H-5), 0.956 (3H, s, H-23), 1.14 (bd, *J* 12.0, H-9), 1.21 (3H, s, H-26), 1.22 (m, H-3), 1.25 (m, H-11), 1.27 (m, H-6), 1.33 (3H, s, H-27), 1.46 (m, H-3), 1.48 (m, H-2), 1.49 (m, H-12), 1.51 (m, H-7), 1.55 (m, H-1), 1.60 (m, H-11), 1.62 (m, H-12), 1.63 (m, H-6), 1.67 (m, H-2),1.69 (3H, s, H-29), 1.80 (m, H-7), 1.81 (2H, m, H-15), 1.811 (3H, s, H-30), 1.82 (3H, s, H-28), 2.24 (2H, t, *J* 7.2, H-19), 2.32 (2H, t, *J* 7.2, H-20), 2.48

(2H, m, H-16), 2.69 (s, O*H*), 3.52 (dd, *J* 11.6, 2.4, H-13), 5.38 (t, *J* 6.8, H-21), 5.50 (t, *J* 6.6, H-17); δ_C 15.67 (C-25), 16.10 (C-28), 17.73 (C-29), 18.34 (C-11), 18.91 (C-2), 20.11 (C-6), 20.80 (C-26), 21.46 (C-24), 21.80 (C-27), 22.77 (C-16), 25.85 (C-30), 27.09 (C-12), 27.22 (C-20), 33.33 (C-4), 33.46 (C-23), 36.79 (C-10), 39.08 (C-1), 39.76 (C-15), 40.24 (C-19), 42.06 (C-7), 42.34 (C-3), 56.24 (C-5), 57.52 (C-9), 73.04 (C-14), 74.51 (C-13), 74.91 (C-8), 125.0 (C-21), 125.7 (C-17), 131.1 (C-22), 134.7 (C-18). EIMS *m/z* (%): 69 (100), 81 (35), 95 (31), 109 (37), 137 (32), 191 (90), 231 (51), 276 (38), 426 ($M^+ - H_2O$, 3). HRFABMS (glycerol) *m/z* (M + H): calcd. for $C_{30}H_{53}O_2$, 445.4046; found: 445.4070. $[a]_D^{25} = -12.9$ (*c* 0.458, $CHCl_3$).

Product 26 (oil). NMR data in C_6D_6 (400 MHz): δ_H 0.791 (3H, s, H-25), 0.840 (m, H-1), 0.866 (3H, s, H-24), 0.870 (m, H-5), 0.958 (3H, s, H-23), 1.21 (m, H-3), 1.23 (m, H-6), 1.357 (6H, s, H-26 & H-27), 1.44 (m, H-3), 1.47 (m, H-2), 1.51 (m, H-11), 1.59 (m, H-15), 1.61 (m, H-9), 1.64 (m, H-2), 1.65 (m, H-12), 1.68 (m, H-6), 1.70 (3H, s, H-29), 1.72 (m, H-7), 1.74 (m, H-11), 1.79 (m, H-1), 1.81 (3H, s, H-30), 1.85 (3H, s, H-28), 1.98 (m, H-7), 2.00 (m, H-12), 2.11 (d, *J* 6.0, O*H*), 2.16 (dd, *J* 13.2, 13.2, 4.8, H-15), 2.26 (2H, t, *J* 6.8, H-19), 2.31 (m, H-16), 2.33 (2H, t, *J* 6.8, H-20), 2.41 (m, H-16), 3.62 (t, *J* 5.4, H-13), 5.39 (t, *J* 6.8, H-21), 5.51 (t, *J* 7.0, H-17),; δ_C 16.14 (C-25), 16.16 (C-28), 17.39 (C-11), 17.75 (C-29), 19.11 (C-2), 21.48 (C-6), 21.50 (C-24), 23.21 (C-16), 24.20 (C-27), 24.69 (C-26), 25.85 (C-30), 27.26 (C-20), 32.97 (C-12), 33.50 (C-4), 33.55 (C-23), 39.39 (C-10), 40.24 (C-19), 40.43 (C-1), 41.71 (C-15), 42.25 (C-3), 44.00 (C-7), 56.64 (C-5), 59.88 (C-9), 74.73 (C-13), 80.44 (C-8), 80.73 (C-14), 125.0 (C-21), 125.7 (C-17), 131.1 (C-22), 134.6 (C-18). ^{1}H NMR data in acetone-d_6 (400 MHz): δ 0.794 (3H, s, H-24), 0.807 (3H, s, H-25), 0.880 (3H, s, H-23), 0.910 (m, H-5), 0. 920 (m, H-1), 1.16 (m, H-3), 1.202 (3H, s, H-27), 1.27 (ddd, *J* 12.4, 12.4, 3.2, H-6), 1.34 (3H, s, H-26), 1.35 (m, H-15), 1.35 (m, H-3), 1.38 (m, H-9), 1.42 (m, H-2), 1.47 (m, H-11), 1.57 (m, H-7), 1.58 (3H, s, H-29), 1.62 (3H, s, H-28), 1.62 (m, H-6), 1.645 (3H, s, H-30), 1.65 (m, H-2), 1.69 (m, H-12), 1.72 (m, H-11), 1.77 (m, H-7), 1.83 (2H, m, H-1 & H-15), 1.85 (m, H-12), 1.96 (2H, t, *J* 6.8, H-19), 2.02 (m, H-16), 2.08 (m, H-16), 2.33 (2H, t, *J* 7.2, H-20), 3.37 (d, *J* 6.0, O*H*), 3.67 (t, *J* 6.0, H-13), 5.10 (bt, *J* 6.8, H-21), 5.16 (t, *J* 6.8, H-17). EIMS *m/z* (%): 69 (100), 81 (47), 95 (42), 109 (51), 136 (47), 191 (90), 231 (18), 235 (13), 250 (11), 276 (18), 426 ($M^+ - H_2O$, 1). HRFABMS (glycerol) *m/z* (M + H): calcd. for $C_{30}H_{53}O_2$, 445.4046; found: 445.4113. $[a]_D^{25} = -22.9$ (*c* 0.142, $CHCl_3$).

Product 27 (oil). NMR data in C_6D_6 (400 MHz): δ_H 0.768 (3H, s, H-24), 0.910 (3H, s, H-23), 1.16 (dd, *J* 12.0, 2.0, H-5), 1.20 (m, H-3), 1.255 (3H, s, H-26), 1.274 (3H, s, H-25), 1.33 (m, H-3), 1.34 (m, H-1), 1.40 (m, H-6), 1.46 (m, H-7), 1.48 (2H, m, H-2), 1.50 (m, H-6), 1.59 (m, H-11), 1.69 (3H, s, H-29), 1.71 (2H, m, H-1 & H-11), 1.73 (3H, s, H-28), 1.74 (m, H-7), 1.81 (3H, s, H-30), 1.83 (3H, s, H-27), 2.21 (2H, m, H-19), 2.25 (2H, m, H-15), 2.30 (2H, m, H-20), 2.33 (2H, m, H-16), 2.49 (m, H-12), 2.69 (m, H-12), 2.76 (d, *J* 5.0, O*H*), 3.43 (ddd, *J* 10.4, 5.0, 2.0, H-10), 5.37 (t, *J* 7.0, H-21), 5.42 (t, *J* 6.8, H-17), 5.53 (t, *J* 6.8, H-13); δ_C 16.11 (C-28), 16.19 (C-27), 16.34 (C-6), 17.73 (C-29), 20.26 (C-2), 20.87 (C-24), 22.39 (C-26), 23.54 (C-25), 25.62 (C-12), 25.84 (C-30), 27.11 (C-16), 27.23 (C-20), 31.28 (C-11), 32.20 (C-23), 33.39 (C-4), 34.83 (C-7), 40.21 (C-15), 40.26 (C-19), 41.62 (C-3), 41.92 (C-1), 54.37 (C-5), 75.11 (C-9), 75.73 (C-8), 79.63 (C-10), 124.9 (C-17), 125.0 (C-21), 125.3 (C-13), 131.1 (C-22), 134.9 (C-18), 135.2 (C-14). The assignments of C-16 and C-20 and those of C-15 and C-19 are interchangeable. EIMS *m/z* (%): 69 (22), 81 (10), 95 (9), 109 (7), 137 (12), 177 (61), 195 (100), 444 (M^+, 3). HRFABMS (glycerol) *m/z* (M + H): calcd. for $C_{30}H_{53}O_2$, 445.4046; found: 445.4120. $[a]_D^{25} = -9.01$ (*c* 0.233, $CHCl_3$).

Product 28 (oil). NMR data in C_6D_6 (400 MHz): δ_H 0.90 (dd, *J* 12.8, 3.0, H-5), 0.91 (m, H-1), 0.951 (3H, s, H-24), 0.951 (3H, s, H-25), 0.990 (3H, d, *J* 7.2, H-26), 1.01 (3H, s, H-23), 1.10 (m, H-9), 1.26 (dd, *J* 12.4, 3.2, H-3), 1.32 (3H, s, H-27), 1.44 (m, H-6), 1.48 (m, H-2), 1.49 (m, H-3), 1.59 (m, H-6), 1.60 (m, H-7), 1.64 (m, H-11), 1.65 (m, H-2), 1.69 (3H, s, H-29), 1.70 (3H, s, H-28), 1.73 (m, H-7), 1.79 (m, H-1), 1.806 (3H, s, H-30), 1.81 (2H, m, H-15), 1.88 (m, H-8), 2.08 (m, H-16), 2.09 (m, H-11), 2.18 (2H, t, *J* 6.8, H-19), 2.25 (m, H-12), 2.27 (2H, m, H-20), 2.40 (m, H-16), 2.46 (m, H-12), 4.06 (s, O*H*), 5.32 (t, *J* 6.6, H-17), 5.35 (t, *J* 6.8, H-21); δ_C 15.43 (C-26), 16.02 (C-28), 16.44 (C-25), 17.71 (C-29), 17.75 (C-6), 18.76 (C-2), 20.44 (C-11), 21.78 (C-24), 22.69 (C-16), 25.78 (C-27), 25.82 (C-30), 27.07 (C-20), 29.79 (C-8), 33.44 (C-4), 33.71 (C-23), 34.38 (C-12), 34.98 (C-7), 38.71 (C-10), 39.68 (C-1), 40.03 (C-15), 40.15 (C-19), 42.35 (C-3), 52.95 (C-9), 56.86 (C-5), 78.60 (C-14), 124.1 (C-17), 124.8 (C-21), 131.3 (C-22), 135.9 (C-18), 214.2 (C-13). EIMS *m/z* (%): 69 (70), 81 (23), 95 (22), 109 (31), 137 (26), 177 (100), 294 (97), 444 (M^+, 1). HRFABMS (glycerol) *m/z* (M + H): calcd. for $C_{30}H_{53}O_2$, 445.4046; found: 445.4115. $[a]_D^{25} = +32.1$ (*c* 0.42, $CHCl_3$).

Product 29 (oil). NMR data in C_6D_6 (400 MHz): δ_H 0.792 (3H, s, H-25), 0.820 (m, H-1), 0.888 (3H, s, H-24), 0.89 (m, H-5), 0.958 (3H, s, H-23), 1.13 (m, H-6), 1.18 (3H, s, H-26), 1.22 (m, H-3), 1.29 (3H, s, H-27), 1.36 (m, H-11), 1.46 (m, H-3), 1.47 (m, H-2), 1.51 (m, H-1), 1.53 (m, H-9), 1.54 (m, H-11), 1.57 (m, H-7), 1.58 (m, H-6), 1.60 (m, H-12), 1.66 (m, H-2), 1.69 (m, H-12), 1.69 (3H, s, H-29), 1.80 (3H, s, H-30), 1.81 (3H, s, H-28), 1.84 (2H, m, H-15), 1.89 (m, H-7), 2.24 (2H, t, *J* 7.2, H-19), 2.32 (2H, m, H-20), 2.51 (2H, m, H-16), 3.76 (dd, *J* 12.4, 2.8, H-13), 5.38 (t, *J* 6.8, H-21), 5.52 (t, *J* 6.8, H-17); δ_C 14.98 (C-25), 15.82 (C-11), 16.12 (C-28), 17.73 (C-29), 18.82 (C-2), 20.42 (C-6), 21.31 (C-12), 21.63 (C-24), 21.74 (C-27), 22.83 (C-16), 25.84 (C-30), 26.54 (C-26), 27.24 (C-20), 33.18 (C-4), 33.50 (C-23), 37.24 (C-10), 39.16 (C-1), 39.75 (C-15), 40.24 (C-19), 42.23 (C-3), 43.40 (C-7), 50.69 (C-9), 56.30 (C-5), 72.98 (C-14), 74.72 (C-13), 74.91 (C-8), 125.0 (C-21), 125.7 (C-17), 131.1 (C-22), 134.8 (C-18). EIMS *m/z* (%): 69 (51), 81 (22), 95 (21), 109 (25), 137 (34), 149 (54), 191 (93), 231 (100), 249 (30), 276 (18), 279 (16), 444 (M^+, 10). HRFABMS (glycerol) *m/z* (M + H): calcd. for $C_{30}H_{53}O_2$, 445.4046; found: 445.4070. $[a]_D^{25} = +14.7$ (*c* 0.16, $CHCl_3$).

Product 30 (oil). NMR data in C_6D_6 (400 MHz): δ_H 1.19 (6H, s, H-23 & H-24), 1.23 (3H, s, H-25), 1.26 (m, H-3), 1.29 (m, H-1), 1.35 (m, H-3), 1.40 (m, H-8), 1.45 (m, H-2), 1.49 (m, H-1), 1.58 (m, H-2), 1.69 (2H, m, H-7), 1.69 (3H, s, H-29), 1.73 (3H, s, H-27), 1.731 (3H, s, H-28), 1.79 (3H, s, H-26), 1.80 (3H, s, H-30), 2.21 (2H, bt, *J* 6.8, H-19), 2.21 (2H, m, H-15), 2.27 (4H, m, H-11 & H-12), 2.30 (2H, m, H-16 & H-20), 2.72 (m, H-8), 3.48 (bd, *J* 10.6, H-6), 5.37 (bt, *J* 6.8, H-21), 5.42 (m, H-17), 5.45 (m, H-13), 5.55 (bt, *J* 6.8, H-10); δ_C 16.10 (C-27), 16.15 (C-28), 16.30 (C-26), 16.45 (C-2), 17.73 (C-29), 21.22 (C-25), 25.85 (C-30), 27.10 (C-20), 27.22 (C-16), 28.09 (C-24), 28.77 (C-12), 28.79 (C-11), 29.79 (C-7), 31.77 (C-1), 32.79 (C-23), 36.62 (C-3), 37.34 (C-8), 40.21 (C-15), 40.21 (C-19), 71.47 (C-4), 75.81 (C-5), 78.94 (C-6), 124.8 (C-10), 124.8 (C-13), 124.9 (C-17), 124.9 (C-21), 131.1 (C-22), 134.9 (C-14), 135.1 (C-18), 135.6 (C-9). The following assignments are interchangeable due to the very close values: C-10/C-13/C-17/C-21, C-11/C-12, C-14/C-18, C-16/C-20, C-27/C-28. EIMS *m/z* (%): 69 (32), 81 (16), 109 (56), 127 (100), 444 (M^+, 3). HRFABMS (glycerol) *m/z* (M + H): calcd. for $C_{30}H_{53}O_2$, 445.4046; found; 445.4029. $[a]_D^{25} = +5.80$ (*c* 0.50, $CHCl_3$).

Product 31 (solid). NMR data in C_6D_6 (400 MHz): δ_H 0.957 (3H, s, H-25), 0.960 (m, H-5), 0.980 (3H, s, H-24), 0.999 (3H, s, H-26), 1.02 (m, H-1), 1.05 (3H, s, H-23), 1.22 (3H, s, H-28), 1.29 (3H, s, H-27), 1.32 (m, H-3), 1.41 (m, H-11), 1.46 (m, H-2), 1.49 (m, H-6), 1.53 (2H, m, H-3 and H-15), 1.55 (m, H-9), 1.59 (m, H-1 & H-11), 1.68 (m, H-16), 1.70 (m, H-6), 1.74 (m, H-2), 1.77 (3H, s, H-29), 1.78 (m, H-13 & H-19), 1.79 (2H, m, H-7), 1.82 (m, H-15), 1.83 (3H, s, H-30), 1.93 (m, H-19), 1.96 (2H, m, H-12), 1.99 (m, H-16), 2.13 (1H, bs, O*H*), 2.35 (m, H-20), 2.47 (m,

H-20), 3.72 (dd, *J* 8.4, 6.4, H-17), 5.45 (t, *J* 6.8, H-21); δ_C 16.25 (C-25), 17.68 (C-29), 18.84 (C-2), 20.03 (C-6), 21.33 (C-11), 21.52 (C-24), 21.99 (C-28), 23.27 (C-20), 24.50 (C-12), 24.50 (C-27), 25.86 (C-30), 26.30 (C-26), 26.45 (C-16), 33.18 (C-4), 33.73 (C-23), 37.40 (C-10), 38.00 (C-7), 38.49 (C-15), 41.32 (C-1), 41.58 (C-19), 42.75 (C-3), 44.66 (C-8), 57.46 (C-5), 59.23 (C-9), 60.83 (C-13), 72.48 (C-18), 82.03 (C-17), 85.95 (C-14), 125.7 (C-21), 130.9 (C-22). The following carbon signals were particularly small and did not clearly appear: C-7, C-8, C-9, C-10, C-12, C-13, C-16, C-17, C-19 and C-27, thus, the chemical shifts (δ_C) were determined by the cross peaks of HMQC or HMBC spectra. EIMS *m/z* (%): 69 (56), 81 (32), 109 (31), 191 (43), 211 (100), 231 (39), 317 (33), 344 (27), 444 (M^+, 10). HREIMS: *m/z* (M^+), calcd. for $C_{30}H_{52}O_2$, 444.3967; found, 444.3971. $[a]_D^{25} = +1.94$ (*c* 0.283, $CHCl_3$).

Product 32 (solid). NMR data in C_6D_6 (400 MHz): δ_H 0.960 (m, H-5), 0.985 (3H, s, H-25), 0.998 (3H, s, H-24), 1.02 (m, H-1), 1.05 (3H, s, H-23), 1.06 (3H, s, H-26), 1.21 (3H, s, H-28), 1.23 (3H, s, H-27), 1.33 (m, H-3), 1.46 (m, H-11), 1.47 (m, H-9), 1.49 (2H, m, H-2 and H-6), 1.53 (2H, m, H-3 & H-15), 1.60 (m, H-16), 1.62 (2H, m, H-1 & H-11), 1.70 (m, H-15), 1.73 (m, H-6), 1.74 (m, H-19), 1.765 (3H, s, H-29), 1.77 (m, H-2), 1.79 (2H, m, H-7), 1.83 (3H, s, H-30), 1.87 (m, H-13), 1.91 (m, H-19), 1.96 (2H, m, H-12), 2.02 (m, H-16), 2.20 (bs, O*H*), 2.40 (2H, m, H-20), 3.71 (dd, *J* 10.4, 4.6, H-17), 5.44 (t, *J* 6.8, H-21); δ_C 16.37 (C-25), 17.72 (C-29), 18.86 (C-2), 20.04 (C-6), 21.41 (C-11), 21.54 (C-24), 21.92 (C-28), 23.29 (C-20), 24.50 (C-12), 25.19 (C-27), 25.86 (C-30), 26.53 (C-26), 26.54 (C-16), 33.20 (C-4), 33.75 (C-23), 37.41 (C-10), 37.87 (C-7), 39.10 (C-15), 41.16 (C-1), 41.75 (C-19), 42.70 (C-3), 44.26 (C-8), 57.46 (C-5), 59.56 (C-9), 60.31 (C-13), 71.61 (C-18), 83.96 (C-17), 85.84 (C-14), 125.7 (C-21), 130.9 (C-22). The carbon signals of C-7, C-8, C-12, C-13, C-14, C-15, C-16, C-17 and C-27 did not appear, thus, the δ_C was determined by the cross peaks of HMBC and/or HMQC spectra. EIMS *m/z* (%): 69 (37), 81 (20), 95 (21), 109 (31), 191 (32), 211 (100), 231 (30), 317 (25), 344 (15), 444 (M^+, 5). HREIMS: *m/z* (M+), calcd. for $C_{30}H_{52}O_2$, 444.3967; found, 444.3978. $[a]_D^{25} = +4.35$ (*c* 0.09, $CHCl_3$).

Product 33 (oil). NMR data in C_6D_6 (600 MHz): δ_H 0.761 (3H, s, H-24), 0.902 (3H, s, H-23), 1.13 (m, H-3), 1.14 (dd, *J* 12.1, 1.5, H-5), 1.23 (m, H-1), 1.236 (3H, s, H-26), 1.30 (m, H-3), 1.309 (3H, s, H-25), 1.37 (dt, *J* 4.8, 13.1, H-7), 1.40 (m, H-6), 1.44 (2H, m, H-2), 1.53 (bd, *J* 12.3, H-6), 1.61 (2H, m, H-11), 1.694 (3H, s, H-29), 1.72 (m, H-1), 1.729 (3H, s, H-28), 1.812 (3H, s, H-30), 1.823 (3H, s, H-27), 1.99 (dt, *J* 4.8, 13.1, H-7), 2.23 (2H, m, H-19), 2.25 (2H, m, H-15), 2.32 (2H, m, H-20), 2.33 (2H, m, H-16), 2.53 (m, H-12), 2.73 (m, H-12), 3.19 (bs, O*H*), 3.63 (dd, *J* 9.9, 2.0, H-10), 5.38 (t, *J* 6.9, H-21), 5.43 (t, *J* 6.5, H-17), 5.51 (t, *J* 6.8, H-13); δ_C 16.08 (C-6), 16.10 (C-27), 16.16 (C-28), 17.75 (C-29), 20.22 (C-2), 20.93 (C-24), 23.49 (C-25), 24.02 (C-26), 25.88 (C-30), 25.91 (C-12), 27.06 (C-16), 27.22 (C-20), 30.63 (C-11), 30.77 (C-7), 32.18 (C-23), 33.35 (C-4), 40.23 (C-15), 40.25 (C-19), 41.36 (C-3), 41.84 (C-1), 54.60 (C-5), 75.51 (C-9), 76.47 (C-8), 77.33 (C-10), 124.9 (C-17), 124.9 (C-21), 125.2 (C-13), 131.1 (C-22), 134.9 (C-18), 135.4 (C-14). The assignments of C-16 and C-20 and those of C-15 and C-19 are interchangeable. The major fragments and their peak intensities in the EIMS spectrum were superimposable to those of **27**. HRFABMS (glycerol) *m/z* (M + H): calcd. for $C_{30}H_{53}O_2$, 445.4046; found: 445.4122. $[a]_D^{25} = 12.7$ (*c* 0.525, $CHCl_3$).

Product 34 (oil). NMR data in C_6D_6 (400 MHz): δ_H 0.735 (3H, s, H-25), 0.77 (m, H-1), 0.889 (3H, s, H-24), 0.89 (m, H-5), 0.957 (3H, s, H-23), 1.14 (dt, 2.0, 12.4, H-9), 1.210 (3H, s, H-26), 1.23 (m, H-3), 1.25 (m, H-11), 1.27 (m, H-6), 1.380 (3H, s, H-27), 1.45 (m, H-3), 1.48 (m, H-2), 1.49 (m, H-12), 1.51 (2H, m, H-1 and H-7), 1.56 (m, H-15), 1.60 (m, H-11), 1.64 (m, H-6), 1.67 (m, H-2), 1.682 (3H, s, H-29), 1.69 (m, H-12), 1.80 (m, H-7), 1.802 (3H, s, H-30), 1.811 (3H, s, H-28), 1.96 (td, *J* 12.7, 4.9, H-15), 2.24 (2H, m, H-19), 2.32 (2H, m, H-20), 2.39 (m, H-16), 2.49 (bs, O*H*), 2.60 (m, H-16), 3.51 (dd, *J* 11.8, 2.2, H-13), 5.37 (bt, 6.8, H-21), 5.52 (t, *J* 7.0, H-17); δ_C 15.67 (C-25), 16.12 (C-28), 17.72 (C-29), 18.41 (C-11), 18.91 (C-2), 20.11 (C-6), 20.78 (C-26), 21.46 (C-24), 22.58 (C-16), 23.58 (C-27), 25.83 (C-30), 26.96 (C-12), 27.22 (C-20), 33.33 (C-4), 33.45 (C-23), 36.79 (C-10), 37.40 (C-15), 39.10 (C-1), 40.24 (C-19), 42.08 (C-7), 42.35 (C-3), 56.24 (C-5), 57.60 (C-9), 73.04 (C-14), 74.94 (C-8), 75.91 (C-13), 125.0 (C-21), 125.8 (C-17), 131.1 (C-22), 134.8 (C-18). The major fragments and their ion intensities in the EIMS spectrum were superimposable on those of **25**. HRFABMS (glycerol) *m/z* (M + H): calcd. for $C_{30}H_{53}O_2$, 445.4046; found: 445.4068. $[a]_D^{25} = 2.20$ (*c* 0.25, $CHCl_3$).

Product 35 (oil). NMR data in C_6D_6 (600 MHz): δ_H 1.153 (3H, s, H-23), 1.200 (3H, s, H-25), 1.216 (3H, s, H-24), 1.23 (m, H-1), 1.24 (m, H-3), 1.35 (m, H-3), 1.48 (m, H-2), 1.63 (m, H-7), 1.64 (m, H-2), 1.693 (3H, s, H-29), 1.735 (3H, s, H-27), 1.735 (3H, s, H-28), 1.75 (m, H-7), 1.77 (m, H-1), 1.788 (3H, s, H-26), 1.805 (3H, s, H-30), 2.24 (2H, m, H-15), 2.24 (2H, m, H-19), 2.27 (2H, m, H-12), 2.27 (2H, m, H-11), 2.32 (2H, H-16), 2.32 (2H, H-20), 2.40 (m, H-8), 2.71 (m, H-8), 2.92 (bs, O*H*), 3.57 (bd, *J* 10.4, H-6), 5.37 (bt, *J* 4.8, H-21), 5.42 (m, H-17), 5.45 (m, H-13), 5.55 (bt, *J* 4.8, H-10); δ_C 16.11 (C-27), 16.17 (C-28), 16.25 (C-2), 16.25 (C-26), 17.72 (C-29), 22.67 (C-25), 25.83 (C-30), 27.13 (C-16), 27.24 (C-20), 27.42 (C-24), 27.88 (C-1), 28.75 (C-11), 28.78 (C-12), 29.00 (C-7), 33.32 (C-23), 36.66 (C-3), 37.52 (C-8), 40.22 (C-15), 40.22 (C-19), 71.73 (C-4), 76.38 (C-5), 77.80 (C-6), 124.87 (C-21), 124.92 (C-13), 124.92 (C-17), 124.97 (C-10), 131.1 (C-22), 134.9 (C-14), 135.1 (C-18), 135.5 (C-9). The following assignments are interchangeable due to the close values: C-10/C-13/C-17/C-21, C-11/C-12, C-14/C-18, C-16/C-20, C-27/C-28. The major fragments and their ion peak intensities in the EIMS spectrum were superimposable on those of **30**. HRFABMS (glycerol) *m/z* (M + H): calcd. for $C_{30}H_{53}O_2$, 445.4046; found; 445.4032. $[a]_D^{25} = -3.03$ (*c* 0.33, $CHCl_3$).

Product 36 (solid). NMR data in C_6D_6 (600 MHz): δ_H 1.014 (3H, s, H-24), 1.032 (3H, s, H-25), 1.066 (3H, s, H-23), 1.100 (3H, s, H-26), 1.17 (m, H-5), 1.20 (m, H-1), 1.271 (3H, s, H-28), 1.371 (very broad singlet, H-27), 1.40 (m, H-3), 1.44 (m, H-11), 1.45 (m, H-16), 1.46 (m, H-13), 1.54 (m, H-2), 1.56 (m, H-3), 1.59 (m, H-6), 1.63 (dt, *J* 5.3, 12.9, H-19), 1.68 (2H, m, H-1 & H-9), 1.70 (2H, m, H-15), 1.70 (m, H-16), 1.70 (m, H-1), 1.71 (m, H-11), 1.73 (2H, m, H-12), 1.78 (m, H-2), 1.80 (m, H-6), 1.825 (3H, s, H-29), 1.846 (3H, s, H-30), 1.89 (dt, *J* 5.3, 12.9, H-19), 1.99 (very broad, H-7), 2.41 (m, H-20), 2.54 (m, H-20), 3.27 (very broad, H-17), 5.45 (t, *J* 7.0, H-21); in acetone-d_6, the signal of H-17 clearly appeared as dd (*J* 11.1 and 3.3), indicating the stereochemistry of C17 is *S*, and O*H* signal was clearly found at 3.83 (brs); δ_C 16.77 (C-25), 18.11 (C-29), 19.05 (C-2), 19.66 (C-28), 20.43 (C-6), 21.50 (C-24), 22.13 (C-11), 22.35 (C-20), 25.13 (C-16), 25.84 (C-30), 26.38 (C-27), 27.32 (C-26), 30.25 (C-12), 33.21 (C-4), 33.78 (C-23), 34.10 (C-15), 37.46 (C-10), 38.94 (C-7), 41.25 (C-1), 42.79 (C-3), 43.00 (C-19), 45.26 (C-8), 56.97 (C-5), 60.28 (C-9), 61.95 (C-13), 73.74 (C-17), 76.01 (C-18), 76.38 (C-14), 126.2 (C-21), 130.7 (C-22). The assignments of C-11 and C-12 are exchangeable. The carbon signals of C-7, C-8, C-12, C-13, C-15, C-16, C-27 and C-28 was significantly small and some peaks did not appear, thus, the δ_C was determined by the cross peaks of HMBC and/or HMQC spectra. ^1H NMR data in acetone-d_6 (600 MHz): 0.807 (3H, s, H-24), 0.823 (3H, s, H-23), 0.832 (3H, s, H-25), 0.92 (m, H-5), 0.920 (3H, s, H-26), 0.97 (m, H-1), 1.13 (m, H-3), 1.15 (3H, s, H-28), 1.24 (m, H-11), 1.324 (s, H-27), 1.33 (m, H-3), 1.35 (m, H-2), 1.38 (m, H-13), 1.42 (m, H-11), 1.42 (m, H-19), 1.43 (m, H-6), 1.47 (m, H-1), 1.52 (m, H-9), 1.55 (m, H-16), 1.58 (m, H-6), 1.62 (2H, m, H-2 & H-6), 1.62 (3H, s, H-29), 1.63 (m, H-12), 1.65 (3H, s, H-30), 1.67 (m, H-19), 1.70 (2H, m, H-15), 1.72 (m, H-12), 1.79 (2H, m, H-7), 2.13 (m, H-20), 2.23 (m, H-20), 3.31 (dd, *J* 11.1, 3.3, H-17), 3.83 (brs, O*H*), 5.11 (bt, *J* 6.8, H-22). The proton signal

of Me-27 was significantly small. δ_C in acetone-d_6, 16.86 (C-25), 18.09 (C-29), 19.24 (C-2), 20.24 (C-28), 20.25 (C-6), 21.54 (C-24), 22.35 (C-11), 22.56 (C-20), 25.46 (C-16), 25.81 (C-30), 26.50 (C-12), 27.10 (C-27), 27.37 (C-26), 33.53 (C-4), 33.84 (C-23), 34.12 (C-15), 37.82 (C-10), 39.30 (C-7), 41.53 (C-1), 43.09 (C-3), 43.37 (C-19), 45.64 (C-8), 57.29 (C-5), 60.56 (C-9), 62.50 (C-13), 73.59 (C-17), 76.72 (C-18), 76.89 (C-14), 126.7 (C-21), 130.9 (C-22). The carbon signals of C-7, C-8, C-11, C-12, C-13, C-15, C-16, C-27 and C-28 was significantly small and some peaks did not appear, thus, the δ_C was determined by the cross peaks of HMBC and/or HMQC spectra. EIMS *m/z* (%): 69 (52), 81 (32), 109 (31), 191 (62), 211 (32), 231 (100), 317 (12), 344 (24), 444 (M^+, 4). HREIMS: *m/z* (M^+), calcd. for $C_{30}H_{52}O_2$, 444.3967; found, 444.3974. $[a]_D^{25} = +29.5$ (*c* 0.78, $CHCl_3$).

References

1 R. B. Woodward and K. Bloch, *J. Am. Chem. Soc.*, 1953, **75**, 2023–2024.
2 J. W. Cornforth, R. H. Cornforth, C. Donniger, G. Popjak, Y. Shimizu, S. Ichii, E. Forchielli and E. Caspi, *J. Am. Chem. Soc.*, 1965, **87**, 3224–3228.
3 (*a*) K. U. Wendt, K. Poralla and G. E. Schulz, *Science*, 1997, **277**, 1811–1815; (*b*) D. J. Reinert, G. Ballianoand and G. E. Schulz, *Chem. Biol.*, 2004, **11**, 121–126.
4 R. Thoma, T. Schulz-Gasch, B. D'Arcy, J. Benz, J. Aebi, H. Dehmlow, M. Hennig, M. Stihle and A. Ruf, *Nature*, 2004, **432**, 118–122.
5 T. Hoshino and T. Sato, *Chem. Commun.*, 2002, 291–301.
6 K. U. Wendt, G. E. Schulz, E. J. Corey and D. R. Liu, *Angew. Chem., Int. Ed.*, 2000, **39**, 2812–2833.
7 (*a*) T. Sato and T. Hoshino, *Biosci., Biotechnol., Biochem.*, 1999, **63**, 2189–2198; (*b*) T. Dang and G. D. Prestwich, *Chem. Biol.*, 2000, **7**, 643–649.
8 T. Hoshino and T. Sato, *Chem. Commun.*, 1999, 2005–2006.
9 C. Pale-Grosdemange, T. Merkofer, M. Rohmer and K. Poralla, *Tetrahedron Lett.*, 1999, **40**, 6009–6012.
10 T. Hoshino, M. Kouda, T. Abe and S. Ohashi, *Biosci., Biotechnol., Biochem.*, 1999, **63**, 2038–2041.
11 C. Pale-Grosdemange, C. Feil, M. Rohmer and K. Poralla, *Angew. Chem., Int. Ed.*, 1998, **37**, 2237–2240.
12 T. Sato, T. Abe and T. Hoshino, *Chem. Commun.*, 1998, 2617–2618.
13 T. Merkofer, C. Pale-Grosdemange, K. U. Wendt, M. Rohmer and K. Poralla, *Tetrahedron Lett.*, 1999, **40**, 2121–2124.
14 T. Hoshino, T. Abe and M. Kouda, *Chem. Commun.*, 2000, 441–442.
15 (*a*) T. Hoshino, M. Kouda, T. Abe and T. Sato, *Chem. Commun.*, 2000, 1485–1486; (*b*) Related paper: S. Schmitz, C. Füll, T. Glaser, K. Albert and K. Poralla, *Tetrahedron Lett.*, 2001, **42**, 883–885.
16 R. Rajamani and J. Gao, *J. Am. Chem. Soc.*, 2003, **125**, 12768–12781.
17 D. A. Dougherty, *Science*, 1996, **271**, 163–168.
18 T. Sato and T. Hoshino, *Biosci., Biotechnol., Biochem.*, 1999, **63**, 1171–1180.
19 C. Füll and K. Poralla, *FEMS Microbiol. Lett.*, 2000, **183**, 221–224.
20 T. Sato and T. Hoshino, *Biosci., Biotechnol., Biochem.*, 2001, **65**, 2233–2242.
21 C. Füll, *FEBS Lett.*, 2001, **509**, 361–364.
22 T. Sato, S. Sasahara, T. Yamakami and T. Hoshino, *Biosci., Biotechnol., Biochem.*, 2002, **66**, 1660–1670.
23 T. Sato, M. Kouda and T. Hoshino, *Biosci., Biotechnol., Biochem.*, 2004, **68**, 728–738.
24 T. Hoshino, S. Nakano, T. Kondo, T. Sato and A. Miyoshi, *Org. Biomol. Chem.*, 2004, **2**, 1456–1470.
25 K. U. Wendt, A. Lenhart and G. E. Schulz, *J. Mol. Biol.*, 1999, **286**, 175–187.
26 T. Hoshino, K. Shimizu and T. Sato, *Angew. Chem., Int. Ed.*, 2004, **43**, 6700–6703.
27 T. Hoshino and T. Kondo, *Chem. Commun.*, 1999, 731–732.
28 T. Hoshino and S. Ohashi, *Org. Lett.*, 2002, **4**, 2553–2556.
29 S. Nakano, S. Ohashi and T. Hoshino, *Org. Biomol. Chem.*, 2004, **2**, 2012–2022.
30 (*a*) H. Tanaka, H. Noguchi and I. Abe, *Org. Lett.*, 2004, **5**, 803–806; (*b*) H. Tanaka, H. Noguchi and I. Abe, *Tetrahedron Lett.*, 2004, **45**, 3093–3096; (*c*) I. Abe, T. Dang, Y. F. Zheng, B. A. Madden, C. Feil, K. Poralla and G. D. Prestwich, *J. Am. Chem. Soc.*, 1997, **119**, 11333–11334; (*d*) Y. F. Zheng, I. Abe and G. D. Prestwich, *J. Org. Chem.*, 1998, **63**, 4872–4873.
31 I. Abe, H. Tanaka and H. Noguchi, *J. Am. Chem. Soc.*, 2002, **124**, 14514–14515.
32 T. Hoshino, Y. Kumai, I. Kudo, S. Nakano and S. Ohashi, *Org. Biomol. Chem.*, 2004, **2**, 2650–2657.
33 G. A. Crispino and K. B. Sharpless, *Tetrahedron Lett.*, 1992, **33**, 4273–4274.
34 J.-L. Abad, J. Casas, F. Sanchez-Baeza and A. Messeguer, *J. Org. Chem.*, 1995, **60**, 3648–3656.
35 W. Aalbersberg and Y. Singh, *Phytochemistry*, 1991, **30**, 921–926; A. Hisham, M. D. Ajitha Bai, Y. Fujimoto, N. Hara and H. Shimada, *Magn. Reson. Chem.*, 1996, **34**, 146–150.
36 A. Chawla and S. Dev, *Tetrahedron Lett.*, 1967, 4837–4843; W. F. Paton, I. C. Paul, A. G. Bajaj and S. Dev, *Tetrahedron Lett.*, 1979, 4153–4154; B. N. Ravi, R. J. Wells and K. D. Croft, *J. Org. Chem.*, 1981, **46**, 1998–2001.
37 E. E. van Tamelen, J. Willet, M. Schwartz and R. Nadeu, *J. Am. Chem. Soc.*, 1966, **88**, 5937–5938.
38 K. B. Sharpless, *J. Am. Chem. Soc.*, 1970, **92**, 6999–7001; K. B. Sharpless, *Chem. Commun.*, 1970, 1450–1451.
39 B. A., Jr. Hess and L. Smentek, *Org. Lett.*, 2004, **6**, 1717–1720.
40 J. W. Cornforth, *Angew. Chem., Int. Ed. Engl.*, 1968, **7**, 903.
41 E. J. Corey and S. C. Virgil, *J. Am. Chem. Soc.*, 1991, **113**, 4025–4026.
42 E. J. Corey, S. C. Virgil and S. Sarsha, *J. Am. Chem. Soc.*, 1991, **113**, 8171–8172.